GOLD THIN-FILM ON POROUS FLEXIBLE POLYESTER MEMBRANE FOR BIO-ELECTRONIC APPLICATIONS

by

Aveek Gangopadhyay
A Dissertation
Submitted to the
Graduate Faculty
of
George Mason University
in Partial Fulfillment of
The Requirements for the Degree
of
Doctor of Philosophy
Electrical and Computer Engineering

Committee:

_____   Dr. Rao V. Mulpuri, Dissertation Director

_____   Dr. Darwin R. Reyes, Committee Member

_____   Dr. Alok Berry, Committee Member

_____   Dr. Qiliang Li, Committee Member

_____   Dr. Nitin Agrawal, Committee Member

_____   Dr. Monson H. Hayes, Department Chair

_____   Dr. Kenneth S. Ball, Dean, Volgenau School
of Engineering

Date: _____   Fall Semester 2016
George Mason University
Fairfax, VA

Gold Thin-Film on Porous Flexible Polyester Membrane for Bio-Electronic Applications

A Dissertation submitted in partial fulfillment of the requirements for the degree of Doctor of Philosophy at George Mason University

by

Aveek Gangopadhyay
Master of Science
Syracuse University, 2007
Bachelor of Engineering
University of Rajasthan, 2005

Director: Rao Mulpuri, Professor
Department of Electrical and Computer Engineering

Fall Semester 2016
George Mason University
Fairfax, VA

DEDICATION

To memory of my late grandparents Bina Ganguly (didi), Anil Ganguly (dadu muni), Sudhir Banerjee (dadu bhai) and Basanti Banerjee (abu maa) who left footprints in my life and to late Honorable President of India, Dr. A. P. J. Abdul Kalam whose success and humbleness have been the source of motivation to me.

ACKNOWLEDGEMENTS

TABLE OF CONTENTS

LIST OF FIGURES

viii

LIST OF ABBREVIATIONS

Alternate current .... AC
Cell growth media.. CGM
Clausius-Mossotti .... CM
Dielectrophoresis .... DEP
Dimethyl sulfoxide.. DMSO
Direct current .... DC
Extracellular matrix .... ECM
Fibronectin .... FN
Fluorescein isothiocyanate.. FITC
Hybrid Cell-adhesive Material.. hCAM
Indium-Tin-Oxide.. ITO
Microelectrode Array.. MEA
Negative dielectrophoresis.. n-DEP
Phosphate-buffered Saline .... PBS
Poly(ethylene glycol).. PEG
Poly(ethylene terephthalate) .... PET
Polyallylamine hydrochloride.. PAH
Polydimethylsiloxane.. PDMS
Polystyrenesulfonic.. PSS
Positive-dielectrophoresis.. p-DEP
R.. Radius
Revolution per minute.. rpm
Scanning electron microscope .... SCM

ABSTRACT

GOLD THIN-FILM ON POROUS FLEXIBLE POLYESTER MEMBRANE FOR BIO-ELECTRONIC APPLICATIONS

Aveek Gangopadhyay, Ph.D.

George Mason University, 2016

Dissertation Director: Dr. Rao Mulpuri

Over the last few decades, there has been a large growth in the development of technologies for neuroscience applications. The majority of these technologies rely on the separation of bio-particles and monitoring bioelectrical responses. To record the bioelectrical activity, patterned electrode arrays have been widely used. Successful results have been obtained on arrays formed on rigid substrates. However, in certain biological/biomedical applications, rigid devices reached their application limit. Flexibility is necessary, in a number of instances, to successfully integrate electronics with specific biological systems. This gives rise to the need of flexible materials, which not only need to be biocompatible but maintain stable electrical properties under mechanical loading conditions.

Rigid Indium-Tin-Oxide based microelectrode array devices have been fabricated; and successfully trapped cells dielectrophoretically. Various electrode array geometries

have been tried in this work. Micro-well electrodes and planar electrodes positioned to trap cells against gravity were used to position the cells at specific locations. Deposition of extracellular matrix and polyelectrolyte layers on the electrodes supported cellular activities. Cells trapped on the functionalized surface remained attached to the electrodes for a long time.

This work also presents, circular-interdigitated gold electrode array devices, which have also been formed and characterized on flexible polyester membrane. When gold electrodes were functionalized with extracellular matrix and polyelectrolyte layers, cells were successfully trapped and cellular growth was also observed over a period of days. Further investigation showed that the presence of pores on the polyester membrane improve the electrical response of the patterned array devices.

This work shows that the porous nature of the polyester reduces the tension drastically, thus meeting the requirement of reliable electrical integrity when subjected to harsh mechanical stress-strain conditions, similar to what a wearable device may encounter. Electrical response to physiologically relevant electrolyte solutions was measured showing the wearable nature of the polyester based electrode array devices. Impedance measurement of the differentiated stem cells on the gold electrodes showed the capability of the electrodes to study cellular properties.

CHAPTER 1: INTRODUCTION

It is a well-known fact that organisms are made up of an extraordinary complex system which consists of tens of thousands of genes, tens of thousands of proteins, RNA molecules and complex organic and inorganic compounds. For a living organism to survive, these components interact in a complex way with each other in their biological environment. This fundamental interaction plays an important role in wound healing, physiology, pathophysiology, and tissue engineering [1]. This extreme complexity of living organisms makes difficult to study and explore even the basic biological processes and functions. To understand this complex interaction various methods and techniques exist that answer various challenges in the study and understanding of cellular-activities and measurement of biomarkers.

1.1 Motivation

For a long time, many research groups have worked on intracellular recording and stimulation technologies using implantable devices (Figure 1.1). Such devices use sharp or patch microelectrodes, to be implanted on to individual neurons. The duration of intracellular recording in this invasive method is limited by mechanical and biophysical instabilities. In contrast, microelectrode array (MEA) device is a promising non-invasive device making significant contribution to the field of bio-sensing. The MEA has achieved a high degree of success in the study of characterization of cells and neural activity [2,
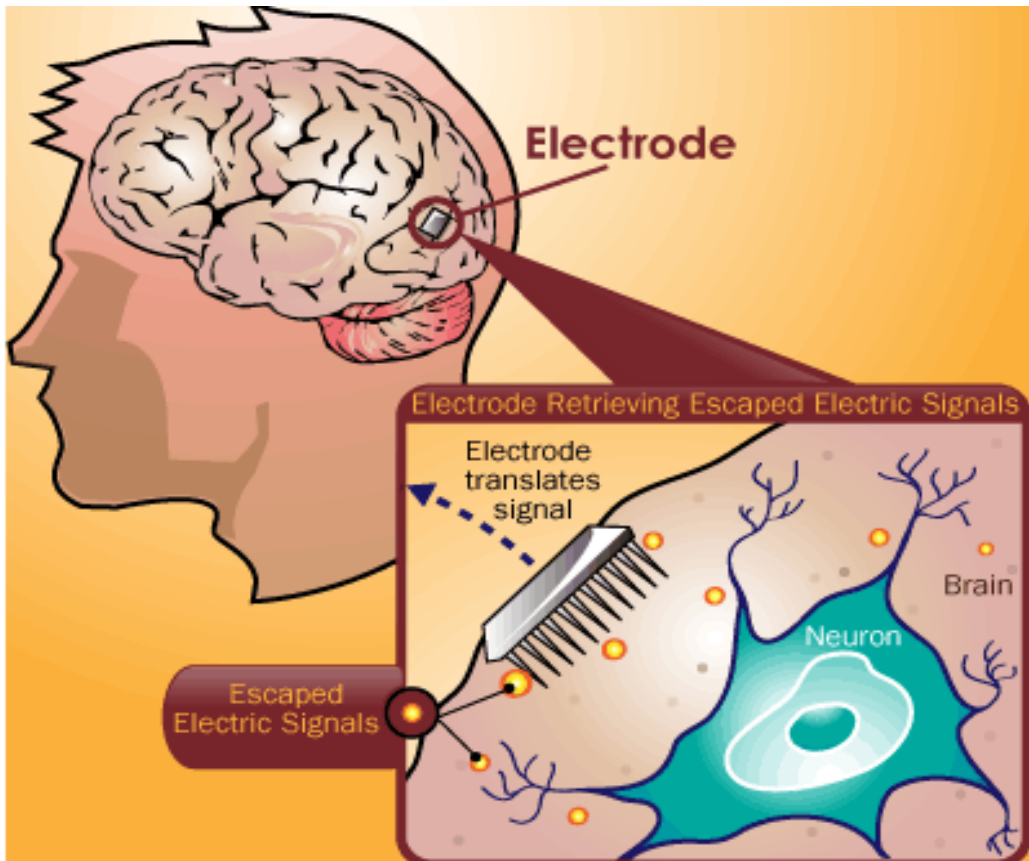
Figure 1.1 A schematic of implantable electrode device in human brain for measuring neuron signals. (Source: HowStuffWorks 2007).

3]. However, most MEAs reported in the literature are rigid substrate devices which find

limited application in some biomedical applications. On the other hand, flexible substrate

could push the limitation boundary further by increasing the scope of applications.

Flexible electronics has a long history. Forty years ago single-crystalline silicon solar

cells were thinned to raise their power and weight ratio for use in extraterrestrial

satellites. Because these solar-cells were thin, they were flexible and warped like corn

flakes. About 20 years ago, ultra-thin, transistors were fabricated on bendable polymer

sheets [4,5]. Flexible electronics is a rapidly developing field of research, whose

boundary is wide-open with many applications.

1.1.1 Biosensors
Cellular behavior is regulated by heterogeneous arrangement of neighboring cells.

Distribution of extracellular matrix (ECM), protein [6-8] and many other factors

influence cellular behavior and functions such as proliferation, differentiation, apoptosis

and migration [9-12]. To artificially reproduce these cellular microenvironments in *in-vitro* experimental conditions, cell-adhesive surfaces and cell-patterns are use practical

approaches [13-20]. *In-vitro* cell culture method, where cells are grown in an artificial

biological environment outside living organism, becomes a basic and primary step of

various research works that allows focus on investigation of smaller microorganisms.

These types of work, where a collection of cells were grown *in-vitro* on bioengineered

surfaces for investigating a variety of fundamental biological activities such as cell-cell

interaction, cell-matrix interaction, proliferation, differentiation and other physiological
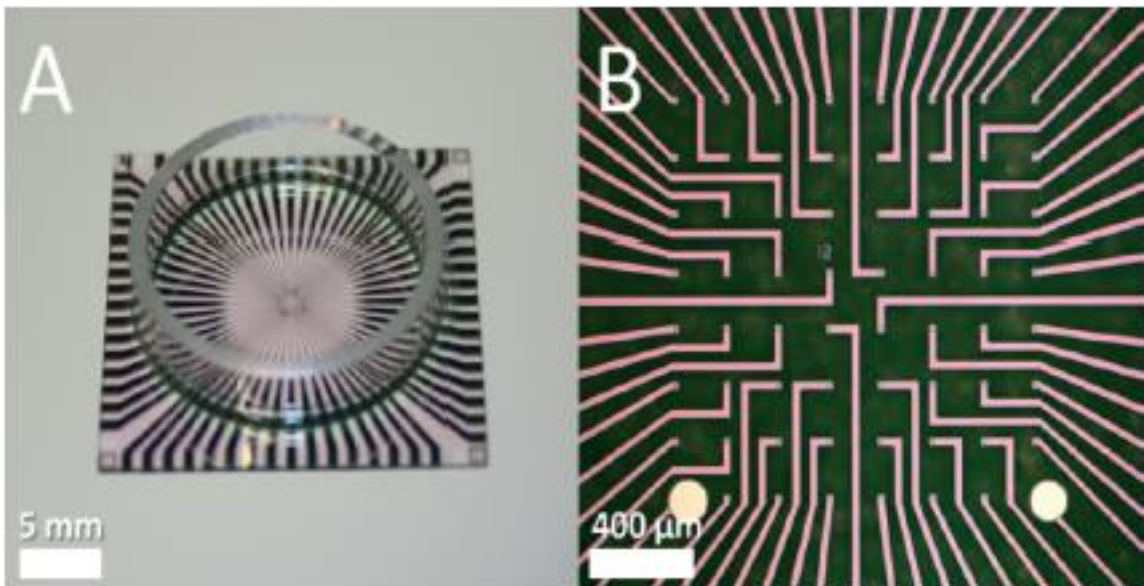
Figure 1.2 Microelectrode array device (Ti/Pt electrodes on Silicate substrate) for recording neuron transmitted signal. (a) Image of the MEA device. (b) Zoomed image of the microelectrodes. (Yakushenko *et al.*, Lab on a Chip, 2014).

behaviors, help simplify the microenvironment and therefore the understanding of such interactions.

Advancement in micro/nano-fabrication technologies such as, photolithography, micro-contact printing, micro-molding, stencil patterning, microchannel patterning, in conjunction with surface chemistry and tissue engineering have led to many novel devices and systems which are used for cell separation, patterning, trapping and culturing. A large number of research work have been reported cells that are separated and trapped on devices [21-23], cultured for extracellular recording and stimulated to detect chemical and biological toxins [24-34]. A number of applications in neuro-technology, pharmacology and cell-based assays make use of MEA (Figure 1.2) for cellular separation and cell-studies [35-40]. Since the development of the first MEA [41–44], technological efforts have improved the quality of information gained by cellular trapping, extracellular recordings. [25,30,45-46] and long-term examination of bio-particles. Various separation technologies such as electrophoresis, chromatography, dielectrophoresis etc. were used to extract target cells and provide control over positioning cells, which is valuable when monitoring, screening, and detectingin a number of biological applications. A number of diagnostic biosensors have been reported to measure bio-particles (biomarkers), *in-vitro and in-vivo*, with precise positioning of cells and high sensitivity, to gain valuable insights into cellular biology at the system level.

1.1.2 Flexible Electronics

Electronics has influenced daily life with such an astounding speed which very few technologies were able to do. Even though microchip industries are still flourishing they face a major challenge when it comes to meeting the demand of wearable biosensors. Requirement of rapid and accurate measurement of biomarkers in cells and bodily fluids limit the application of commercially available biosensors. Current electronic devices are limited to tracking an individual's physical activities and vital signs only. Gaining an insight on the state of health of an individual is beyond the scope of rigid or semi-flexible biosensors because it requires real-time, continuous, precise monitoring of biomarkers and physiological relevant substances at molecular levels. Unconventional flexible and stretchable wearable electronics is the way to achieve these objectives (Figure 1.3 and Figure 1.4). [47-53]. Next generation wearable devices are required not only to be highly flexible and stretchable but also to obtain precision and stable electrical response under harsh stress-strain conditions.

1.2 Scope of Current Work

In chapter 2, results on MEA devices with different electrode geometries formed on rigid and flexible substrates are presented. Electrode surfaces were functionalized to enhance the cellular attachment and activities. Cells were positioned on the electrodes by applying dielectrophoresis force. Trapped cells adhered to the functionalized surfaces of the electrodes. Under proper culture conditions, long-term cellular growth and activities were monitored in a microfluidic environment on the flexible devices.

Figure 1.3 A wearable device for real-time perspiration analysis during cycling. (Source: Gao et al., Nature, 2016).

Figure 1.4 Stretchable Silicon circuit wrapped on a finger. (Roger et al. Science, 2010).

In chapter 3, a new type of flexible polyester material with gold electrodes is discussed which not only takes the existing wearable technology to a new level but also maintains stable and reliable electrical behavior under extreme mechanical loading conditions. Such materials should not be limited by individual's activities in daily life. These wearable electronic devices have capabilities to monitor an individual's activities, without interrupting or limiting the user's activities or motions [54-62] and are becoming more and more prevalent and a critical tool for real-time, continuous monitoring of body fluids containing biomarkers [63]. For example, a recent study had shown that, specifically, eccrine gland sweat could provide metabolic information not previously thought possible, [64] therefore making the measurement of this body fluid highly valuable to monitor the health of a person. In addition to high degree of flexibility and stretchability, the gold electrodes formed on the polyester material studied in this work shows highly reliable and stable mechanical and electrical properties, thus overcoming many of the challenges encountered by current wearable technologies. When the flexible gold electrodes were bent and twisted, the electrodes were found to be intact and a stable conductivity was measured. Potentiometric measurement of the electrode, in presence of different electrolyte solution, showed the capability of the flexible device to response to ionic changes. These results show the possibility of this porous flexible device to be used as a wearable device.

In chapter 4, results on the cell-impedance were presented to evaluate the capability of the electrodes to detect attached bio-particles. Stem cells were plated on the flexible devices for differentiation. Measurement of the electrodes showed a variation in

impedance with respect to cell-free electrodes. Thus, cellular characterization is possible on the flexible devices.

CHAPTER 2: DIELECTROPHORETIC TRAPPING OF CELLS IN A MICROFLUIDIC SYSTEM

In general, when a spatially non-uniform AC electric field is applied on a dielectric particle suspended in a dielectric medium, a dipole moment is induced on the particle. This polarized particle experiences a force and moves along the electric field line. This phenomenon is called dielectrophoresis, (DEP). Depending upon the relative dipole moment induced on the particle with respect to the medium, polarized particle may either migrate towards sites of maximum field intensity (positive DEP or p-DEP) or away from the sites of maximum field intensity (negative DEP or n-DEP) [21, 65-67]. There are several important reasons to use AC fields for DEP. In a conductive medium, AC fields of sufficient frequency (> 10 kHz) do not suffer from ionic screening or electrode polarization as ions cannot move fast enough to screen the applied field. The movement of particles due to net charge (electrophoresis) will time average to zero in an AC field and electroosmotic flow of the double layer (cell membrane and dipole layer) along liquid (media) – solid (particle membrane) boundaries is eliminated.

For DEP positioning of bio-particles, a conductive on-chip cellular-solution that enable DEP manipulations is required. An imbalance in particle and media conductivities creates the DEP force by a relation known as Clausisu Mossotti (CM) factor [68-69]. The n-DEP requires a high conductive in-system solution to create negative DEP, whereas a p-DEP requires a low conductive in-system solution to create
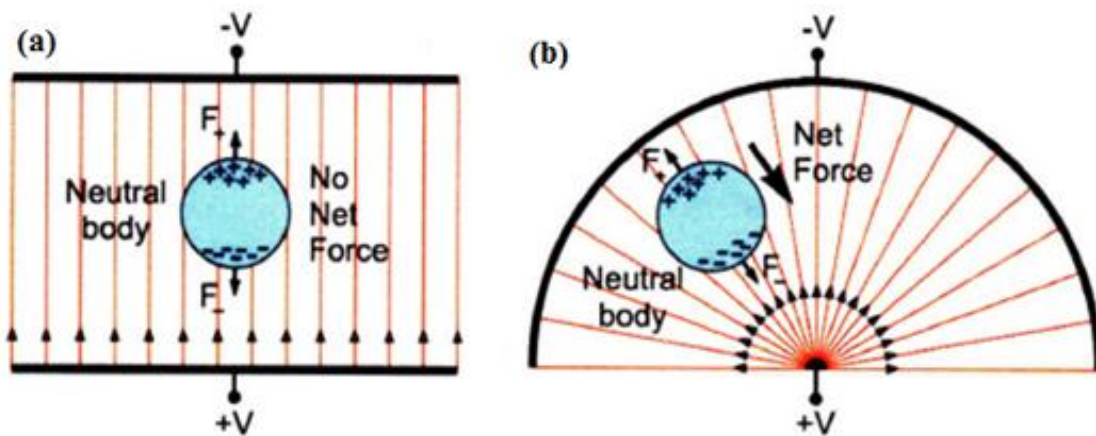
Figure 2.1 Dielectrophoresis force on of a charged particle in (a) Uniform electric field. (b) Non-unifrom electric field. (Source: Brain M. Taff, PhD. Thesis, 2008).

positive DEP. High conductive solution for the p-DEP offers a number of advantages over the n-DEP which include such as low in-system Joule heating effect, a stronger electric-field gradient and a stable attraction-based DEP trapping. In this work, a number of devices have been fabricated that use p-DEP force for positioning the cells.

2.1 Theory of Dielectrophoresis Force

To understand the underlying DEP mechanics, an example of electrode configuration is shown in figure 2.1. A neutral particle is positioned between a set of parallel plates. On applying opposite voltages on the plates, the particle will experience no net electromotive force. In figure 2.1a, the negatively charged electrode attracts positive charges to the top membrane of the particle that mirror the negative charges attracted to the bottom membrane facing the positive charged electrode. In this setup, induced opposite charges perfectly balance each other generating a case of $F^+ = F^-$. Since there is no net electromotive force acting on the particle, the particle shows no tendency of any migration and simply maintains its position between the electrodes. In figure 2.1b, however, the neutral particle is positioned between electrodes of different geometry. Thus, on applying opposite voltages to the electrode plates, a non-uniform electric field is created inducing asymmetric charges within the particle, generating a net electromotive force. In this environment, the particle migrates either along the electric field gradient or opposite to the gradient, depending upon the relative permittivity of the particles with respect to that of suspending medium and also the frequency at which the electrodes are driven.

For a spherical particle inside the non-uniform field, DEP force, as described by Pohl [70], is expressed as

$$F = 2\pi\varepsilon_{media}R^3 Re[CM]\nabla|E_{rms}|^2 \qquad (2.1)$$

where E_{rms} represents rms value of the electric field, ε_{media} represents electrical permittivity of the suspending medium surrounding the particle, R is the radius of the particle, CM represents the complex Clausius-Mossotti factor, which is given by

$$CM = \frac{\varepsilon^*_{particle}-\varepsilon^*_{media}}{\varepsilon^*_{particle}+2\varepsilon^*_{media}} \qquad (2.2)$$

Here ε^* is complex permittivity given by

$$\varepsilon^* = \varepsilon - j\frac{\sigma}{\omega}, \qquad (2.3)$$

where σ denotes electrical conductivity and ω denotes angular frequency of the applied AC electric field and j represent the imaginary term of the expression. This relation is derived from Laplace equation for a particle-media system [71]. The CM factor is the only term in the equation that incorporates frequency of the applied signal. Mathematically, CM factor varies between -0.5 and 1. For a given set-up, when this CM value is positive p-DEP force is observed and when CM value is negative n-DEP force is observed.

In general, Equation 2.1 is an accurate descriptor of DEP force which only accounts for the presence of electrically-induced dipole. But occasionally, discrepancies arise between this model and experimental behavior of the submerged particle in conductive media. This is due to the presence of a variety of higher order charge multipoles in the particles which contribute to overestimating the DEP force, depending

on the topology in the electric field gradient. Higher order multipoles in these particles become more relevant when electric field presents spatial variation over length scales comparable to particle size.

2.2 Fabrication of Microelectrodes Array Devices and Microfluidic System

Microfluidic devices have been used extensively for cell-based assays and to manipulate them inside the channel networks DEP and other trapping techniques have been used [72-74]. Such devices, fabricated using microfabrication technologies, allow precise patterning and manipulation of bio-particles, and thus haves the potential for individual characterization, detection and assay of the trapped cells. Combined with surface chemistry, microfluidic devices are patterned to contain cell adhesive and non-adhesive regions [75-78]. The strategy of confining bio-particles in these microfluidic devices consists of fabricating MEA devices, assembled with a PDMS based microfluidic channel. In this work, a variety of DEP devices have been designed and fabricated. A PDMS microchannel assembled on the devices are then used under different cell-trapping conditions. These MEA designs are capable of handling large number of cells at a time. These devices successfully trapped cells.

2.2.1 Micro-well based MEA device

The first MEA design of the study was aimed at DEP trapping of cells in a device with a micro-well. Glass coated with 1 µm thick Indium-Tin-Oxide (ITO) is used as the substrate. Using photolithography processes, ITO microelectrodes were etched. This design consisted of an array of 60 microelectrodes (10 µm wide each), forming 29 pairs
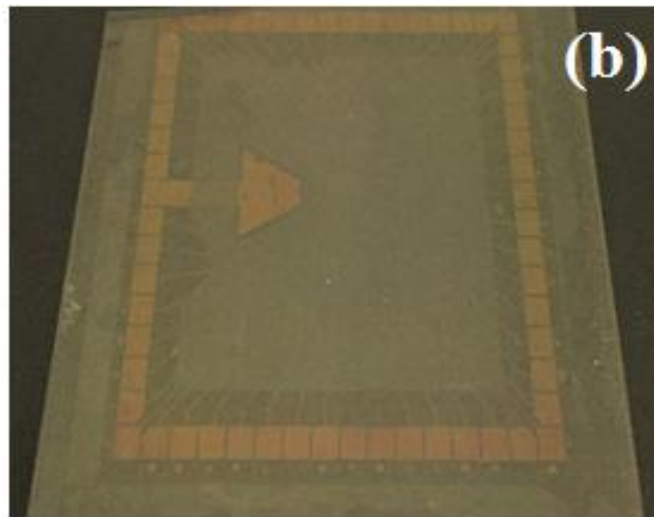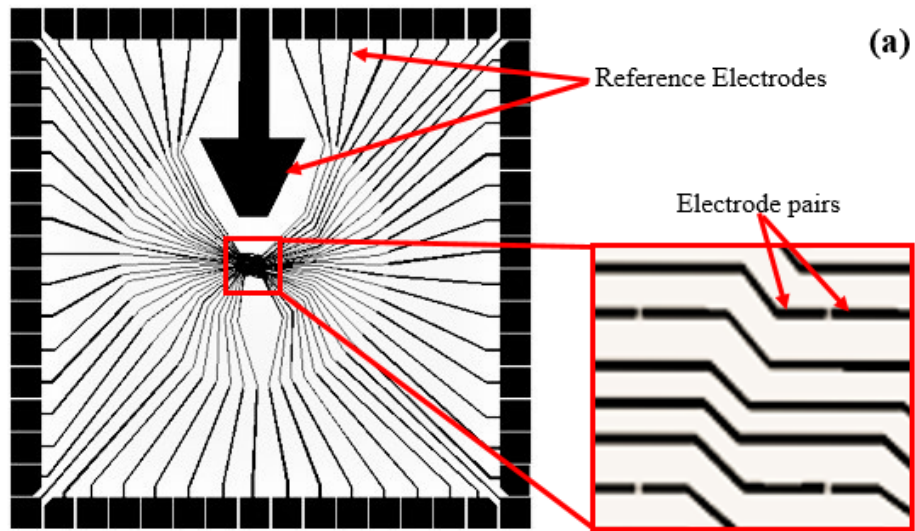
Figure 2.2 Micro-well based MEA (a) Schematic design. (b) Photograph of fabricated device.
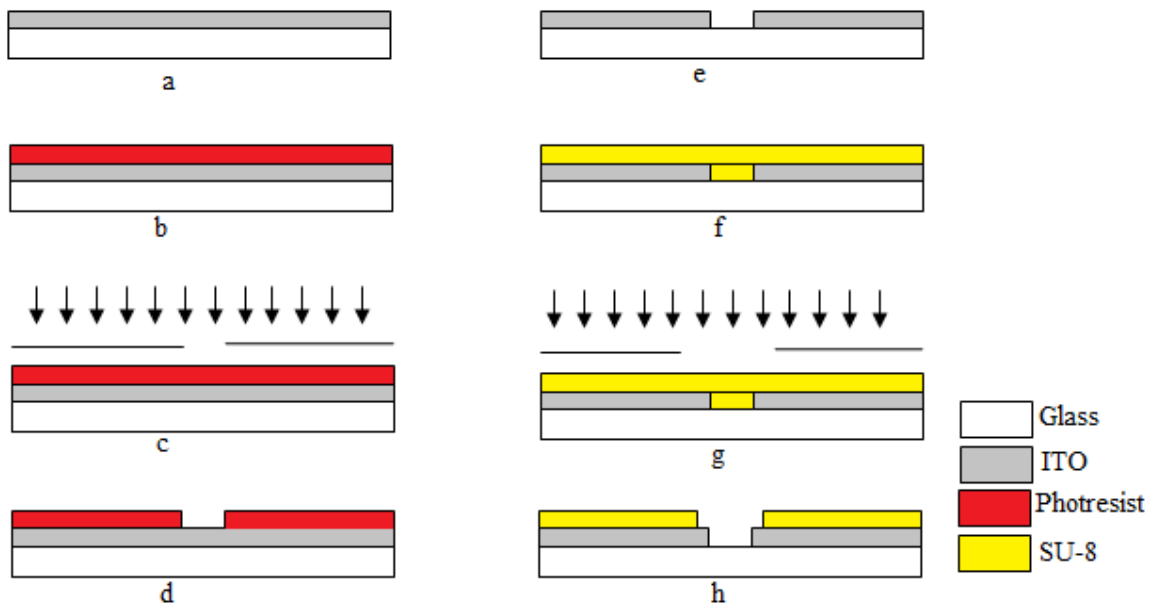
Figure 2.3 Schematic of the fabrication steps of micro-well based MEA device (a) ITO coated glass. (b) Photoresist spin-coated. (c)Photoresist exposed. (d) Development of exposed sample. (e) Etched of developed sample. (f) SU-8 spin coated. (g) SU-8 exposed. (h) Development of exposed SU-8.
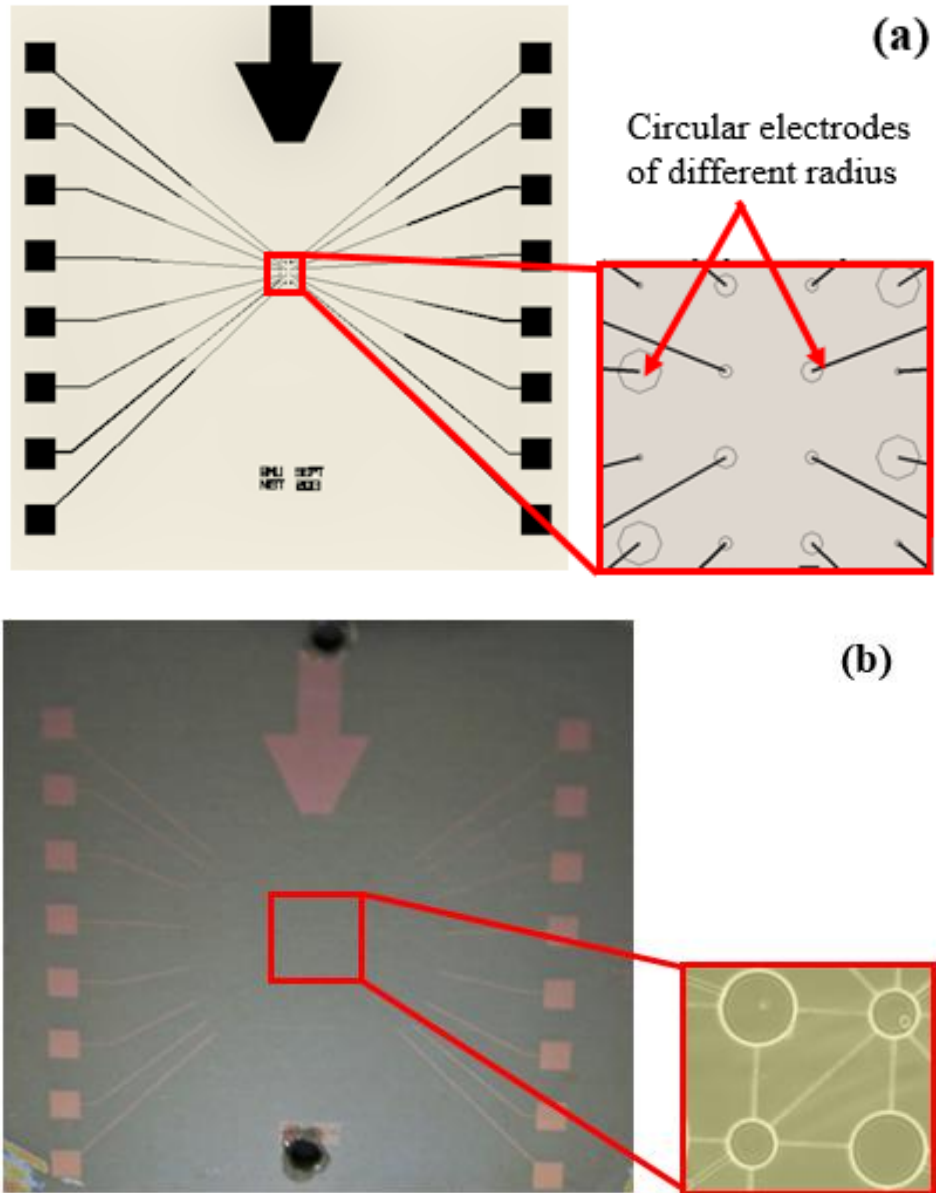
Figure 2.4 Planar MEA device (a)Schematic design. (b) Photograph of a fabricated device.
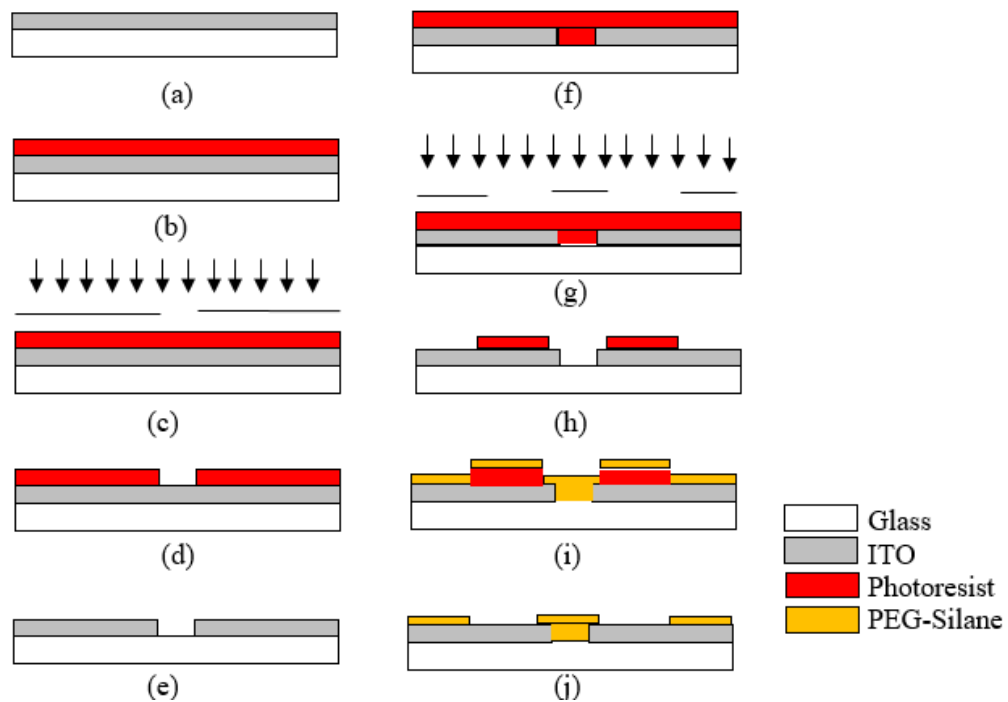
Figure 2.5 Schematic of the fabrication steps of Planar MEA device (a) ITO coated glass. (b) Photoresist spin coated. (c)Photoresist exposed. (d) Development of exposed sample. (e) Etched of developed sample. (f) Photoresist spin coated. (g) Photoresist exposed. (h) Development of exposed sample. (i) PEG-Silanization. (j) Photoresist removal.

of electrodes, 10 µm apart, and 2 ground electrodes (Figure 2.2). Figure2.3 shows the

fabrication steps. In fabricating the device image reversible photoresist, AZ 5214E (4000

rpm, 2000 acceleration for 40 sec) was spin-coated, exposed (60 mj/cm^2), baked, and

flood exposed. The exposed substrate was developed and ITO electrode tracks were

etched. The etched substrate was then spin-coated with SU-8 organic resist, which acts as

an insulator, and exposed to obtain the patterned micro-wells. These micro-wells were

patterned over the regions where a pair of ITO electrodes faced each other to act as cell

trapping locations. The capability of this design to generating a strong DEP force was

verified by a COMSOL simulation previously performed [79].

2.2.2 Planar MEA Device for Trapping Cells Against Gravity

Second MEA design was aimed at trapping the cells at the surface of the MEA

device, placed upside down i.e. in an attempt to trap the cells against gravity. This design

consisted of 16 ITO circular microelectrodes at the MEA surface and 1 blanket ITO

coated ground reference electrode formed on a different substrate and placed under the

flow of cell-media. Figure 2.4 shows the second MEA design and the fabrication steps

are shown in figure 2.5. Tor fabricate the MEA device, photoresist S1813 was spin-

coated (4000 rpm, 1000 acceleration for 45 sec) and exposed (120 mj/cm^2) followed by

the development of exposed resist and etching of the ITO electrode-tracks. Next, the

MEA surface was silanized with poly(ethylene glycol) (PEG), a non-adhesive cellular

material, except the circular electrode surfaces. PEG decreases the attractive force

between solid surfaces and proteins in the cell-membrane. To silanize the MEA surface,
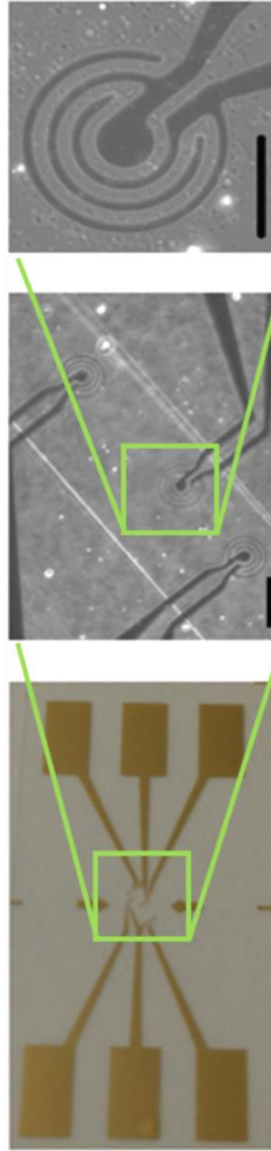
Figure 2.6 Flexible MEA on Polyester membrane.

the etched ITO MEA was spin-coated, as described previously, and exposed and developed with electrode surfaces coated with photoresist. The MEA device was then immersed in a PEG solution which was adsorbed onto the surface. In acetone, the photoresist was removed from the non-silanized ITO electrodes.

2.2.3 Flexible MEA Device on Polyester Membrane

The third MEA design was aimed at trapping cells against gravity, on the surface of an upside down flexible MEA device. The poly(ethylene terephthalate) (PET) polyester membrane was purchased with the track-etched pores. In this design, a 50 nm gold layer was deposited and 10 µm concentric interdigitated gold electrodes were patterned using lift-off low temperature photolithography process and e-beam evaporation methods (Figure 2.6). Gold was selected for this part of the work due to its better conductivity properties compared to the ITO.

2.2.4 Microfluidic Channel

Next, a microfluidic channel was fabricated which was assembled on the MEA devices. Soft-lithography is the key process for fabricating the microfluidic channels. A bio-compatible organic polymer, polydimethylsiloxane (PDMS), which is an inert, non-flammable, non-toxic and optically clear material, was used. To form this microfluidic channel, first an inverse structure of the channel was patterned using SU-8 photoresist on a silicon wafer as a master mold. PDMS pre-polymer was mixed with the curing reagent as per vendor protocol and poured over the master-mold, and then degassed in vacuum chamber before curing overnight at 60 °C. Cured PDMS was then peeled from the master-mold, cut in proper shape and size, and inlet-outlet holes were punched for

(a) Silicon

(b) SU-8 Photoresist spin coated

(c) Exposed

(d) Develope

(e) SU 8 mold on Silicon wafer

(f) Cured SU 8 Mold

(g) PDMS over SU 8 mold

(h) Microfluidic Channel

SU-8
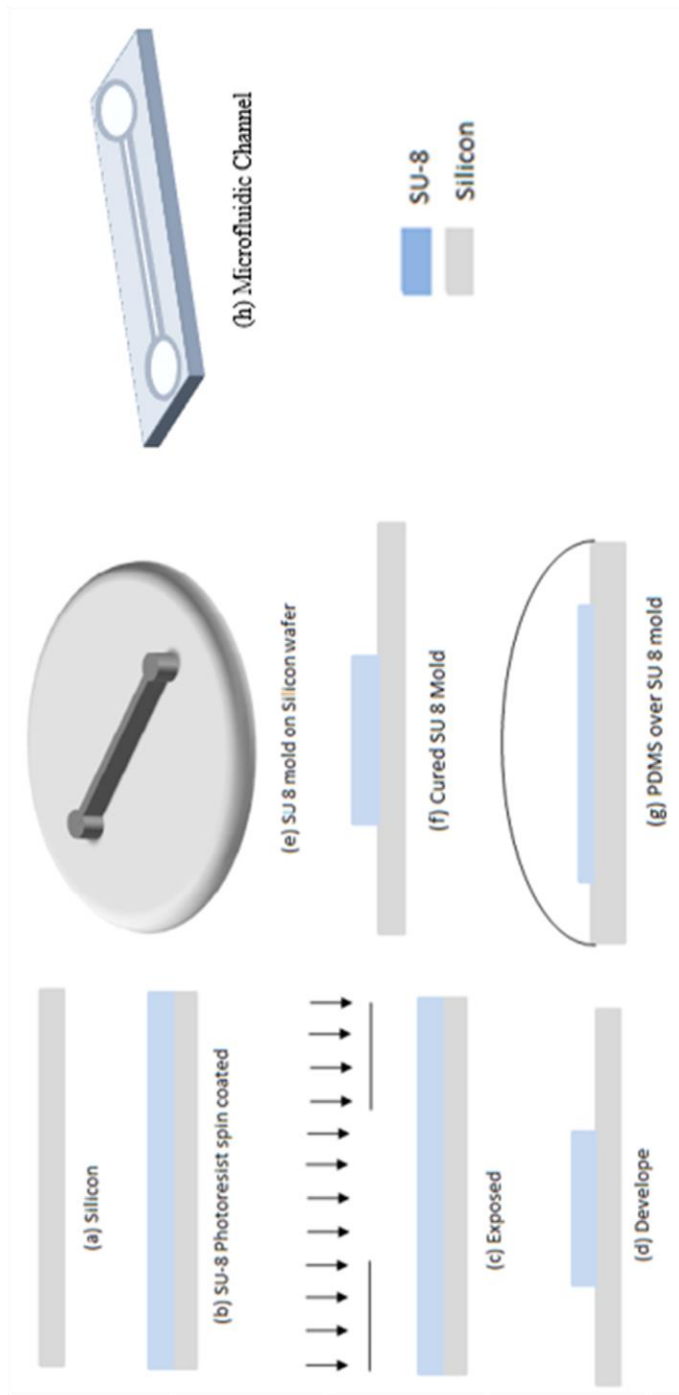
Silicon

Figure 2.7 Schematic of the fabrication steps of microfluidic channel (a) Silicon wafer. (b) SU-8 resist coated. (c) SU-8 resist spin-coated. (d) Exposed SU-8 resist developed. (e) Negative SU-8 tensile. (f) Cured master mold. (g) PDMS poured over master. (h) Peeled and cut PDMS microfluidic channel.
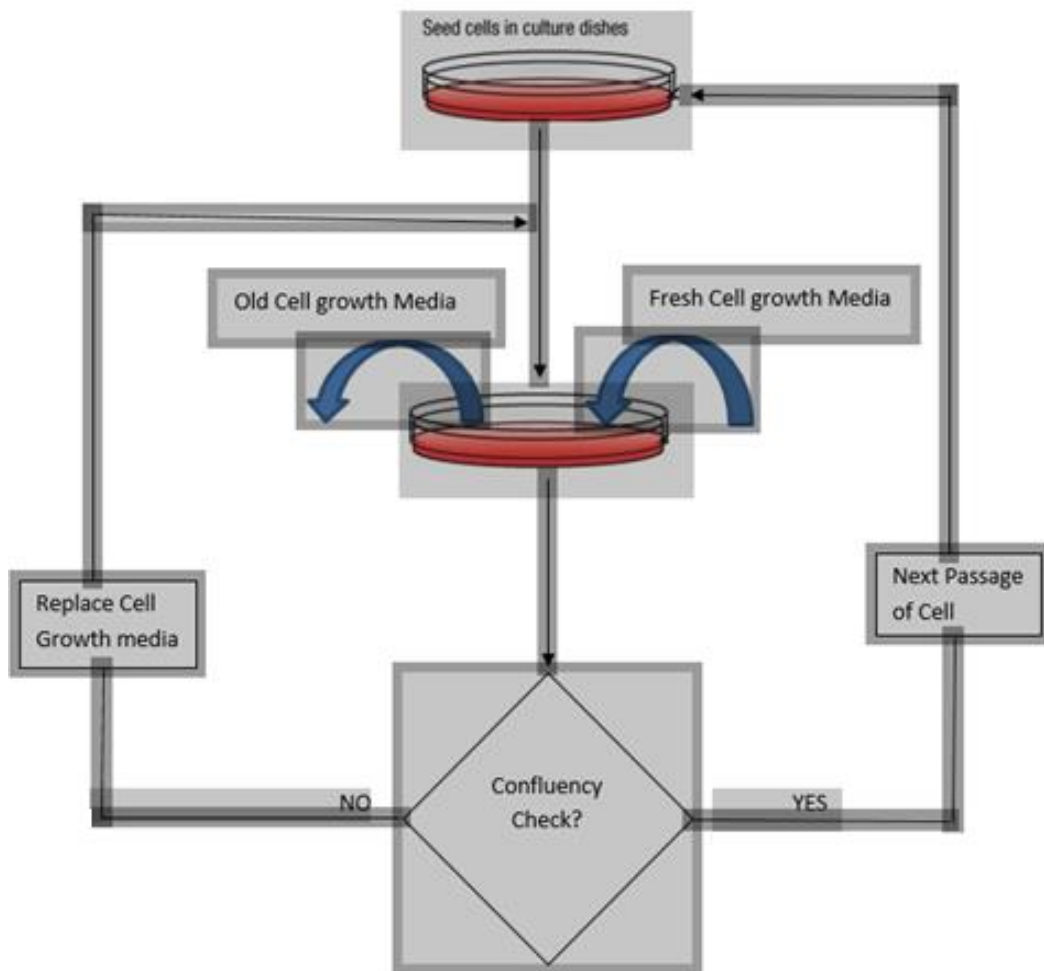
Figure 2.8 Schematic of cell culture protocol.

channel accessibility. Figure 2.7 shows the fabrication process of the PDMS

microchannel. The PDMS was then attached on the MEA device surface such that the

microelectrode array was aligned within the PDMS channel.

2.3 P19 Cells Culture

P19 pluripotent stem cells were the cells chosen for the DEP trapping

experiments. P19 cells are embryonic carcinoma cell line derived from teratocarcinoma

in mice following transplantation of a 7.5-day embryo into testis. The tumor, arose from

the transplanted embryo grew rapidly. Culture of this undifferentiated stem cells was

established from the primary tumor. This cell line is pluripotent and can differentiate into

cell types of any of the germ layers. For the DEP experiment, P19 cells were cultured and

passaged in a treated cell-culture flask with vented cap. This cell line was cultured in cell

growth media (CGM) supplemented with bovine (2.5%) and calf (7.5%) serums.

Supplemented media was replaced with fresh media every 48 hours, supplemented media

was replaced with fresh media. Care was taken to maintain a monolayer of cells

throughout the passage cycle and they were detached for next passage using trypsin

media before reaching 100% confluency (preferably around 80%), in order to maintain

monolayer cell-growth. Figure 2.8 shows the flow chart of the cell-culture protocol that

was followed. Cultured cells were stored in an incubator which was set at 37 °C in 5%

CO_2.

In order to optimize cell growth, the cells were also cultured on a gelatin coated

surface and also under hypoxia conditions (98% CO_2-N_2 mixture). For every 48 hours,

hypoxia cell-culture flask was refilled with CO_2-N_2 gas. A difference was observed in
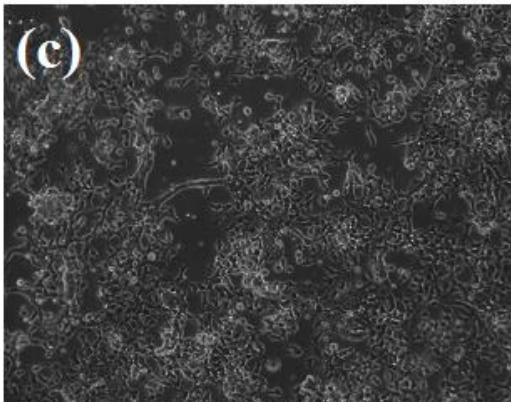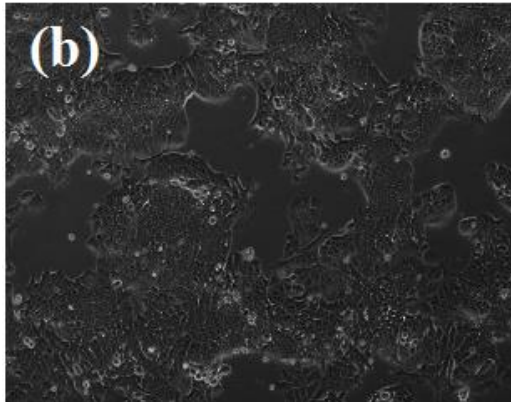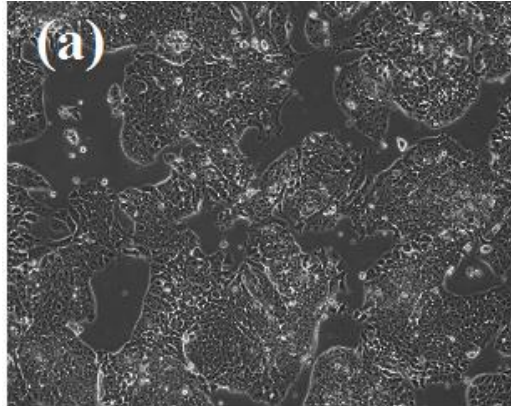
Figure 2.9 Microscope images of cell growth on (a) flask with filter cap. (b) gelatin treated surface. (c) hypoxia condition.
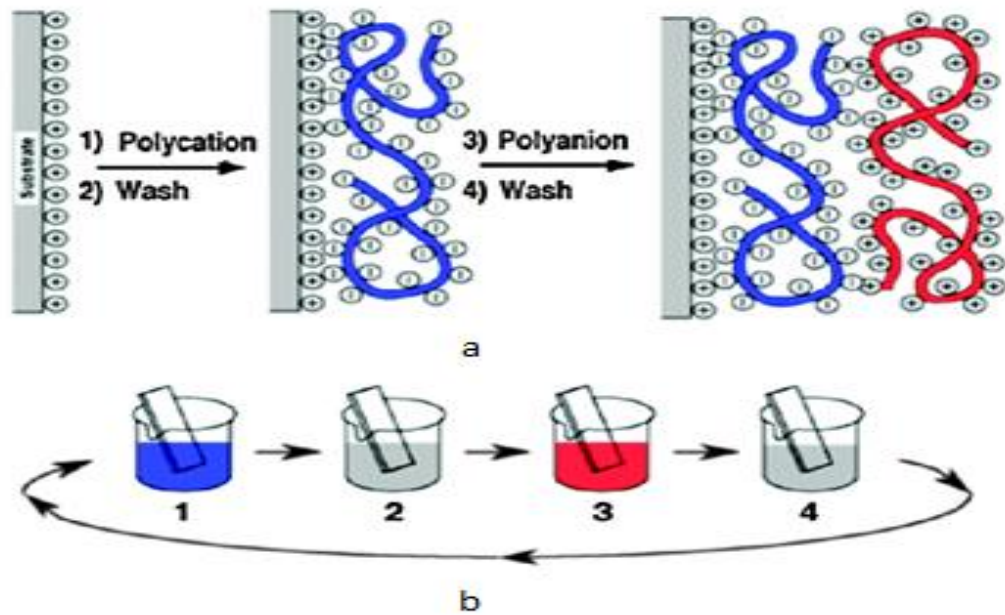
Figure 2.10 Schematic of sequential deposition (a) Adsorption of cationic and anionic charges during layer-by-layer adsorption of polyelectrolytes. (b) Sequential submersion of sample for layer-by-layer adsorption of PEM. (Tang *et. al.*, Adv. Mater., 2006).

growth rate and morphology in different culture conditions. Growth rate was observed to be faster on gelatin surface, whereas in hypoxia conditions cells formed tightly packed cell-colony, but the growth rate was slower as compared to cells on vented tissue culture flask. Figure 2.9 shows the morphology of cell growth under different cell culture conditions.

2.4 DEP Experiment Set-up

2.4.1 Functionalization of Surface

In order to create a bio-compatible environment for the trapped cells, the surface of the MEA device was functionalized. A hybrid cell adhesive material (hCAM) was deposited by filling the microfluidic channel with ionic solutions and extracellular matrix in sequential order. Cationic and anionic layers were formed by layer-by-layer deposition of polyallylamine hydrochloride (PAH) and polystyrenesulfonic (PSS) acid solutions at a concentration of 1 mg/ml in distilled water. These ionic solutions created a strong electrically charged surface on which the polarized cells, once trapped under DEP force, remained attached strongly. Fibronectin (FN), an extracellular matrix protein that binds the cellular membrane via integrin receptors, was deposited on top of the ionic layers, thus mediating the cellular growth process. FN solution was prepared in a Dulbecco's Phosphate Buffer Solution (DPBS) at a concentration of 50 µg/ml. On top of FN adsorbed layer, another layer of PAH was deposited. Always, the top terminating layer is charged positively so that the net negative charges surrounding the cells would mediate, within the first few minutes, a strong attachment onto the surface. Figure 2.10 shows the sequential layer-by-layer deposition of solutions on the MEA surface.
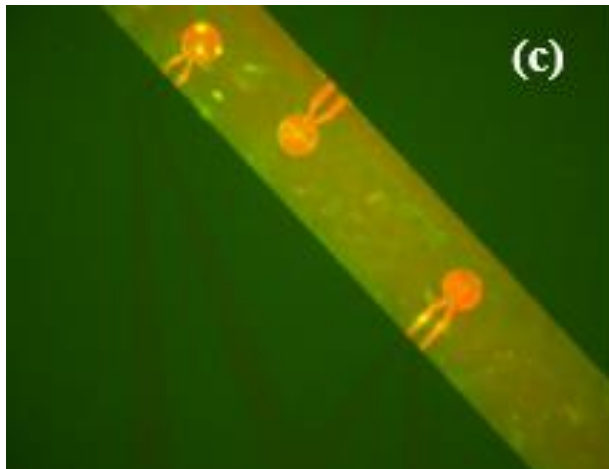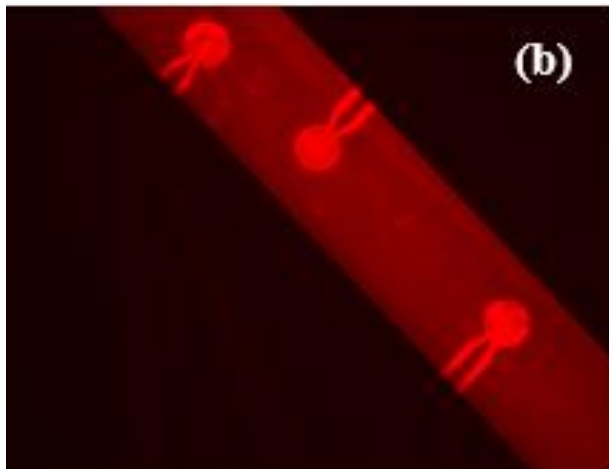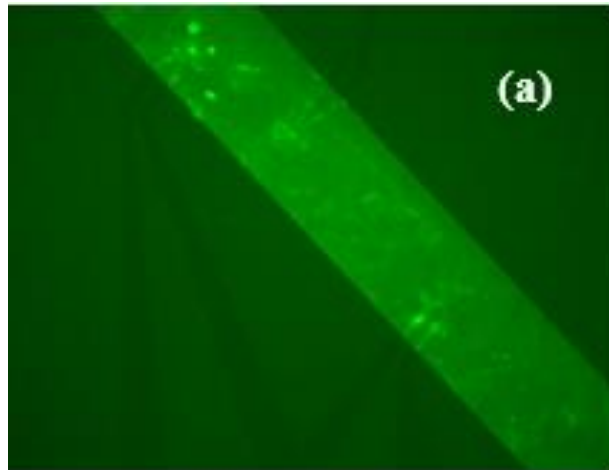
Figure 2.11 Images of fluorescent labelling of hCAM layers (a) PAH-FITC. (b) FN. (c) Overlapped layers of PAH and FN.

The adsorption of hCAM layer was examined by immunostaining the FN and using a PAH tagged with fluorescein isothiocyanate (FITC) in microfluidic channel and imaging the channel/electrode using fluorescence microscopy. The PAH was stained with PAH-FITC for 45 mins, rinsed with water and blocked at ambient temperature for 30 mins. The FN was stained with a primary antibody for 45 mins, rinsed with PBS-Tween and blocked for 30 mins, followed by secondary antibody deposition for another 45 mins and finally rinsed with PBS-Tween. All fluorescent labeling was deposited on top of adsorbed layers, at the ambient temperature. Images were taken (Figure 2.11) after refilling the channel with PBS-Tween. The green color shows homogenous adsorption of PAH-FITC on the surface and red color denotes the homogenous adsorption of FN inside the microfluidic channel. The orange-green color shows the overlapping of FN and PAH layers on the surface.

2.4.2 Cells Positioning

Next, the PDMS channel was filled with 0.32 M sucrose solution in ultra-pure water, pre-warmed at 37 °C. The microfluidic system (MEA device and PDMS microfluidic channel) was connected to an arbitrary waveform generator and placed under a microscope. Cells were detached from culture flask, transferred to a tube and centrifuged (800 rpm, for 5 mins at 4 °C). Without disturbing the cell pellet, formed at the bottom of the centrifuges tube, cell-media was replaced completely with pre-warmed sucrose solution. The cell-pellet was broken into single cells by gently tapping the conical tube. The cell-sucrose solution was aspirated to the inlet-hole of the microfluidic channel. Upon microscopic observation, when cells flow over the electrodes (in micro-well MEA)
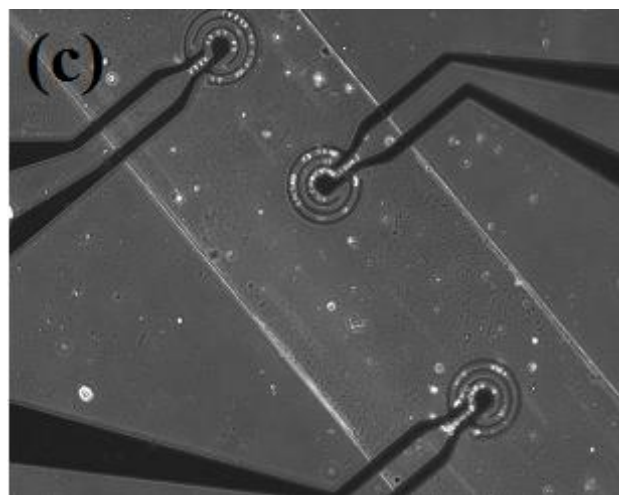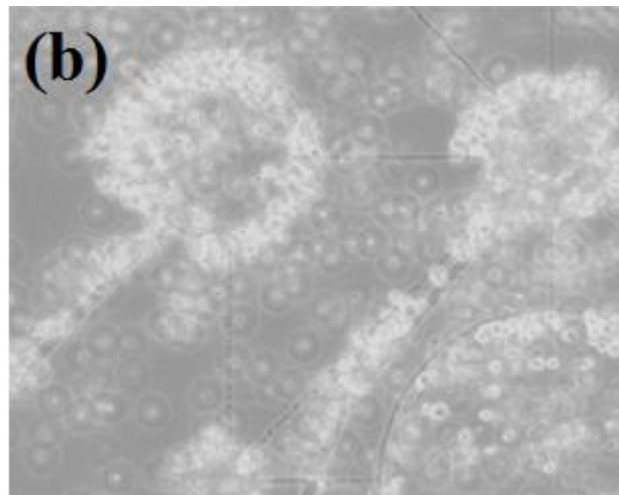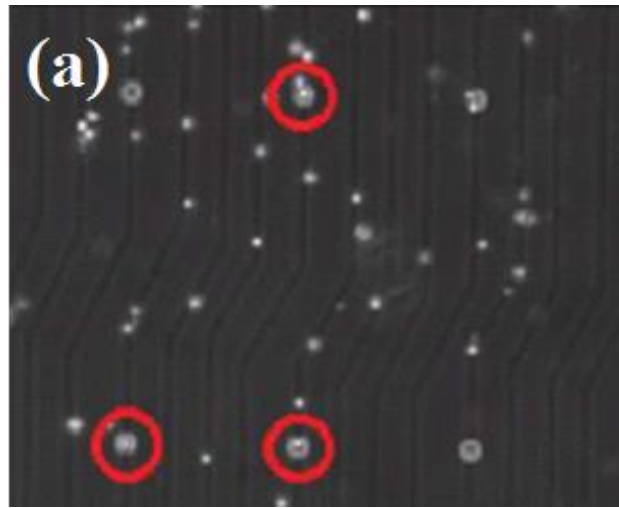
Figure 2.12 Image of Trapped Cells on MEA (a) Micro-well-MEA. (b) planar MEA. (c) Flexible MEA.
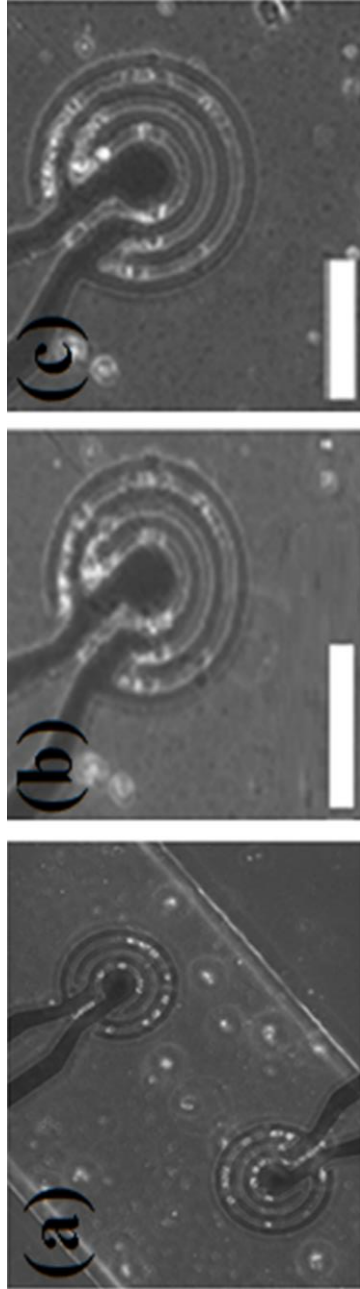
Figure 2.13 DEP Trapped cells on device after (a) 3 hours. (b) 24 hours. (c) 48 hours (scale bar 100 μm).

or underneath the electrodes (on MEA designed for cell-trapping against gravity), the electrodes were energized, thus beginning the p-DEP cell trapping. Figure 2.12 shows the images of DEP trapped cells on the MEA devices. Once sufficient number of cells were trapped, DEP was turned-off. The trapped cells remained adhered to the electrodes even after turning-off the DEP, due to the presence of hCAM which binds the cells to the electrode surface.

2.5 Growth of Trapped Cells in the Microfluidic System

After successful DEP trapping of cells, the sucrose solution in the channel was replaced with supplemented CGM. Adhered cells did not flow away media during the exchange of media. The microfluidic system with trapped cells were stored in an incubator set at 5% CO_2 and 37 °C. The media in the channel was replaced with fresh media every 12 hours. Trapped cells on the flexible MEA (PET/Au device) showed cellular growth. Images were taken for upto 48 hours when the cells stopped showing growth behavior (Figure 2.13).

2.6 Conclusion

Cells were trapped successfully on the fabricated MEA devices, by applying DEP force on ITO electrodes on rigid glass and gold electrodes on flexible polyester. Deposition of hCAM layer improved the adhesion of cells, even against the gravity. Functionalization of surface with extra-cellular matrix protein, like FN, maintained a bio-compatible surface for cellular functionality. Maintaining a suitable bio-environment for the trapped cells in microfluidic channel helped the cells to grow *in-vitro*. Physiological

behavior of the cells and cellular response to various drugs can be studied in detail on these MEA designs.

CHAPTER 3: ELECTRICAL PROPERTIES OF GOLD ELECTRODES FORMED ON POROUS FLEXIBLE POLYMER MEMBRANE

Latest advances in micro- and nano-electromechanical systems have made possible the proliferation of flexible electronic materials. Wearable sensors, [63-64, 80] foldable displays, [81-83] flexible solar cells [84-85] and flexible electronic fibers [86-87] are some of the major areas where flexible electronic technologies are of great interest. Any material when thinned becomes flexible. Today, electronic devices and integrated circuits are thinned so that it does not break when subjected to accidental fall or bend. Flexible can have many attributes: bendable, conformably shaped, rollable, elastically stretchable, non-breakable. The field is open topic and its boundaries move with development and application.

3.1 Challenges of Flexible Electronics

In general, a large area electronics is composed of a substrate, back-plane integrated circuits and encapsulation. All the components must comply with bending to some degree to make the structure flexible. Challenge arises at the requirement that the flexible devices must maintain their electrical and mechanical integrity when bent, twisted, folded, stretched, compressed, or deformed in any other way in order to demonstrate suitable performance. It is known that electrical properties of thin films are influenced significantly by changes in mechanical loading conditions. Properties of thin films formed on flexible substrates have been reported, [88-90] but as new technologies

35

and applications emerge, work on new materials is constantly required. Three types of

substrates that are commonly considered for flexible applications are thin glass, metal

foil, and polymers. However, flexible glass is fragile and difficult to handle while metal

foil is brittle [91] and has limitations of withstanding multiple bend cycles. [92] The

flexible nature of polymeric substrates makes them of significant importance as a

material for practical flexible electronics [93].

3.2 PET/Au under Mechanical Loading

In this work, the effect of stress and strain was compared on the conductivity of

Au films deposited on thin films of the polyester poly(ethylene terephthalate) (PET), with

and without pores, to assess their capabilities as a future component in wearable

electronic devices. Both the PET membranes (porous and non-porous) are approximately

11 μm thick. The porous membranes contain pores with an average diameter of 1.2 μm at

an average density of 10^5 cm^{-2}. Patterned layer of 50 nm thick Au electrodes was

deposited on the PET membranes as described previously in chapter 2. Scanning Electron

Microscopy (SEM) image of porous PET/Au is shown in Figure 3.1. (Image of the

transparent PET is not clear due to reflection of light during SEM imaging). The

patterned membranes were subjected to different radii of curvature (R = 1 - 5 mm) of

convex bending with respect to the Au patterned side. The SEM images of the Au

electrode on PET membranes before (Figure 3.2) and after (Figure 3.3 and Figure 3.4)

mechanical loading are shown. Bending the non-porous PET completely fractured the Au

film along the width of the electrode thus breaking its continuity which was confirmed by

the complete loss of electrical conductivity. Optical image of the complete fracture along
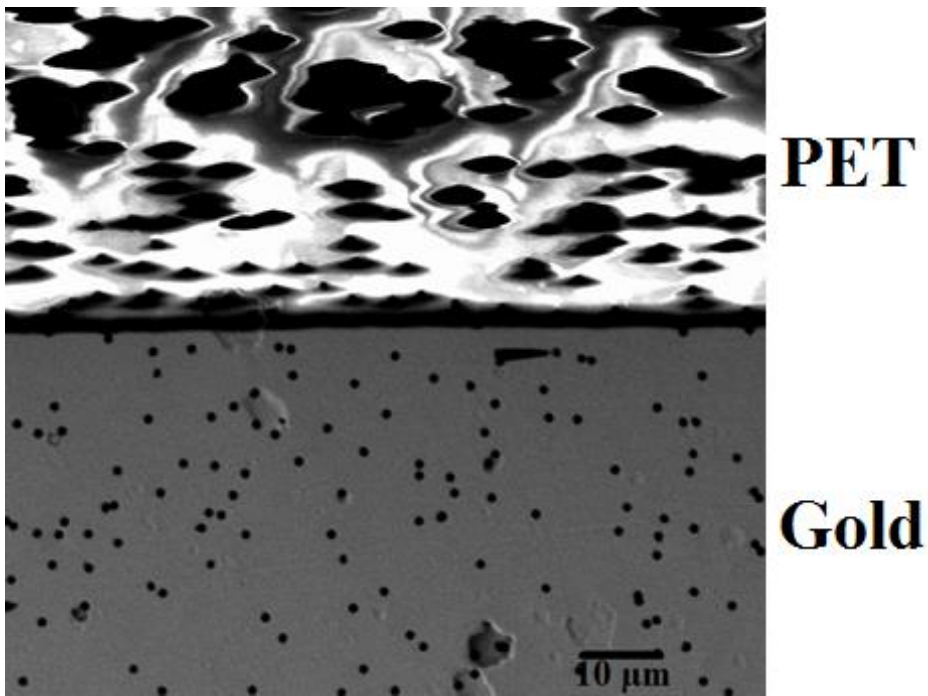
Figure 3.1 SEM Image of porous PET and deposited Gold layer.
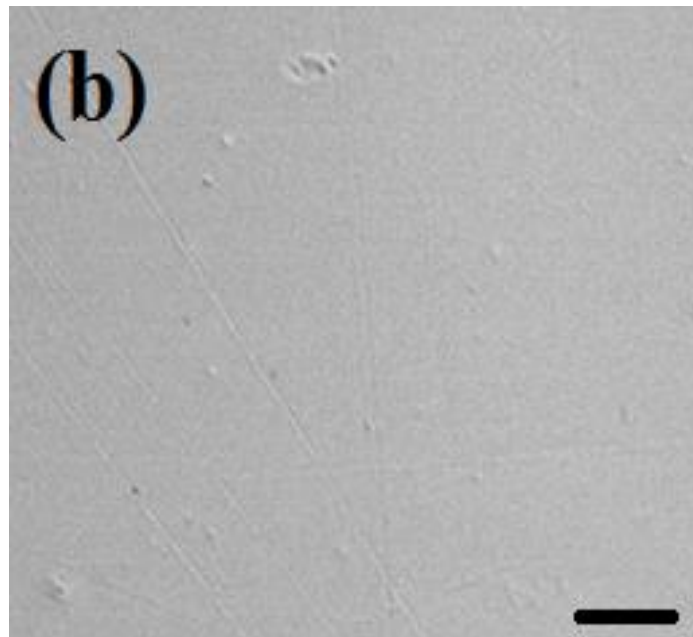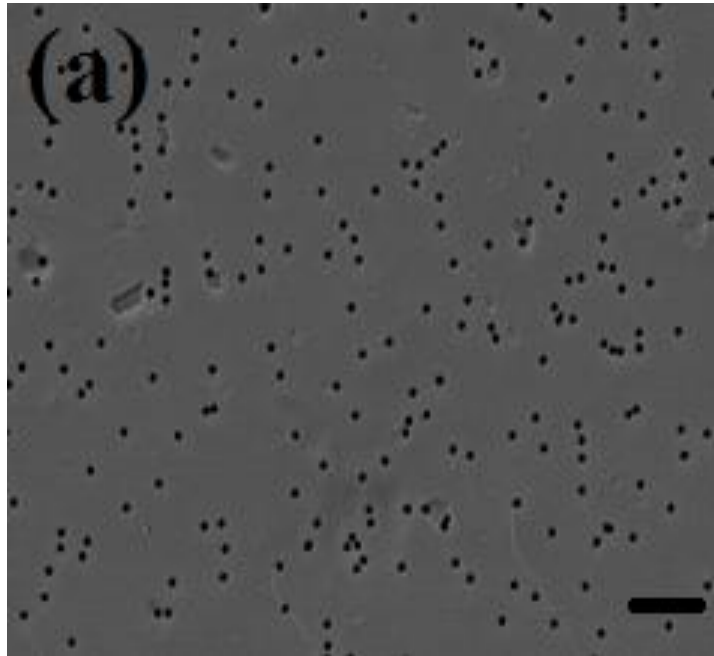
Figure 3.2 SEM Image of Au film before mechanical loading on (a) Porous PET. (b) Non-porous PET. (Scale bar 10 μm).
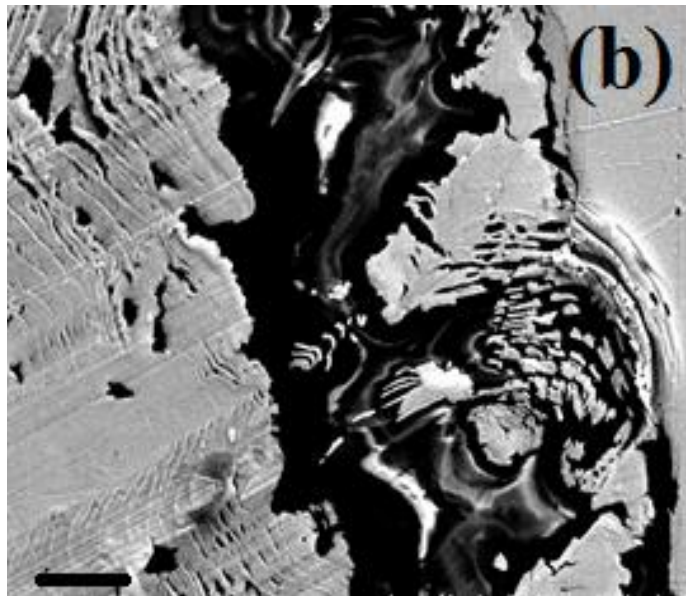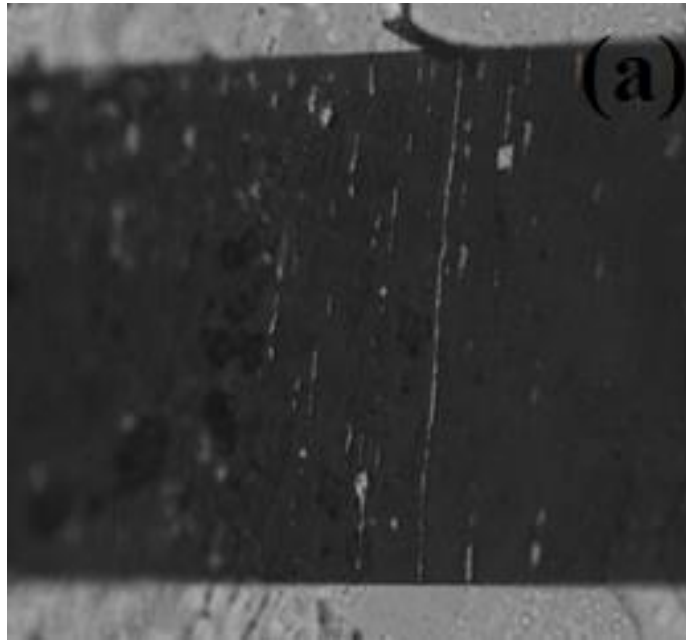
Figure 3.3 Fractured Au film on non-porous PET (a) Optical image taken at 20x. (b) SEM image. (Scale bar 10 μm).
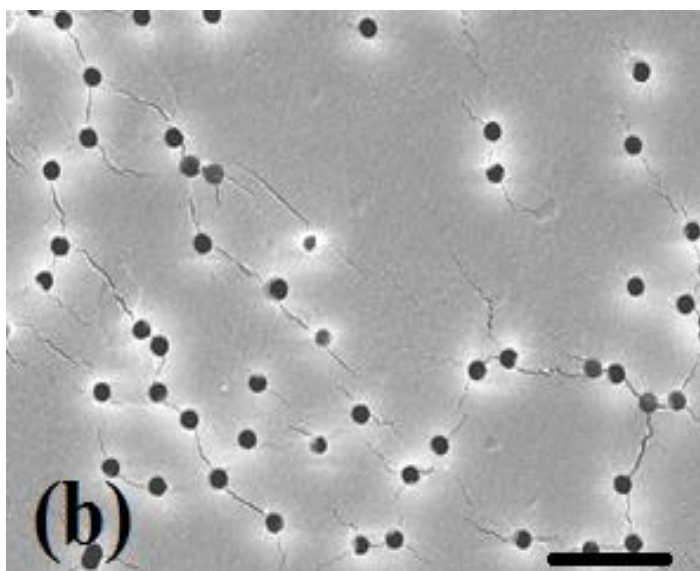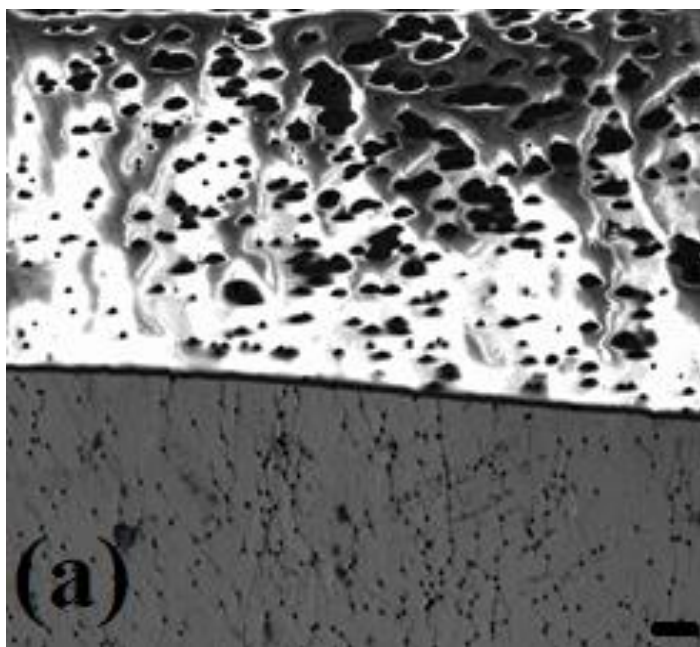
Figure 3.4 SEM Images of cracked Au film on porous PET after mechanical loading (a) PET/Au Image. (b) Only Au image. (Scale bar 10 μm).

the width of the electrode is shown in Figure 3.3. No further characterization was

possible with the Au thin films deposited on the non-porous PET membrane. Bending the

porous PET, however, did not result in catastrophic damage, but only generated small

surface cracks (Figure 3.4) that did not completely penetrate nor disrupt the continuity of

the film. Having pores drastically reduces the tension in the PET membrane so that a

hard, creasable polymeric film becomes readily foldable upon itself and conforms to

objects. Therefore, the porous PET membrane becomes a compliant substrate that

increases the ability of the Au thin-film to withstand mechanical loading and high stress-

strain conditions while maintaining reliable electrical properties

3.3 Conductivity of PET/Au

In order to measure electrical properties and reliability, the conductivity of the Au

film electrodes on the porous PET membrane was measured as a function of bias voltage

and frequency under various mechanical loading conditions. When flexible membranes

are bent, twisted, or folded, the stress and strain are translated to the thin-film it supports,

which in turn affects the mobility of the electrons and extended line-defects on the

surface of the Au films, and ultimately influences conductivity [94-97]. Applied stress

also affects grain boundary migration and coalescence, and the grain size, which is

known to influence the mobile carriers within Au films [98-100]. In general, the mobility

decreases with increasing stress, which consequently decreases the conductivity of the Au

film through the relationship,

$$\sigma = nq\mu \qquad\qquad (3.1)$$
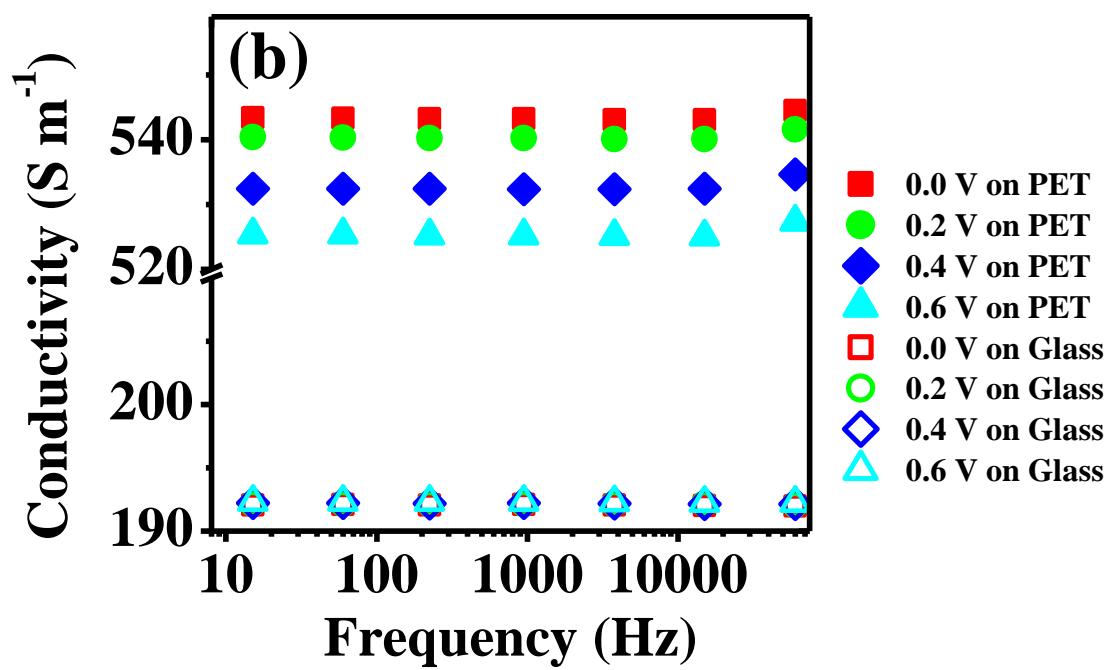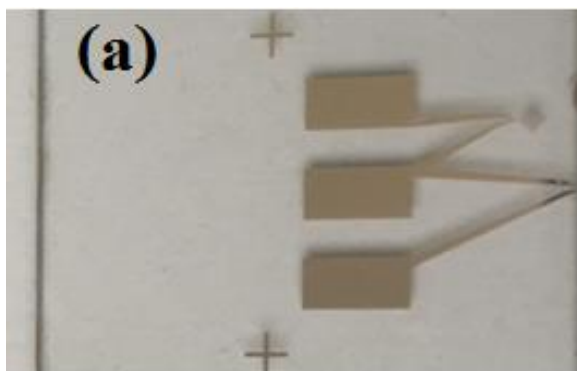
Figure 3.5 Au film on glass (a) Au film on glass substrate. (b) Conductivity of Au film on porous PET membrane and glass substrate.

where σ is conductivity of the film, n is the concentration of electrons, q is the charge of an electron and μ is the mobility of electrons. The conductivity calculation is based upon the assumption of a uniform cross sectional area over the entire length of the Au film. However, the effective cross-sectional area may depend upon the defects in the Au film, such as the holes in the metal film propagated from the pores in the underlying substrate. The gap of the gold layer on the pore walls vary with the applied stress [93]. With bending of the PET membrane, cracks were formed on the surface. The combination of changing the inner pore-wall gap size and the formation of cracks may vary the effective cross-sectional area of the film. The variation in the conductivity with stress is believed to be due to the variation in the electron mobility [100] (Au grain boundaries and defects affect the electron mobility), although the effective cross-sectional area may also contribute to the conductivity variations.

The conductivity of Au electrodes on flat porous PET membrane was compared with Ti/Au electrode on a rigid glass. Since Au does not adhere to the glass, a 5 nm Ti layer is deposited prior to depositing the Au layer. It is found that the conductivity on the PET membrane/Au thin-film electrode was 250% greater than that of Ti/Au on a glass substrate (Figure 3.5). The difference in conductivity on the rigid glass is due to a relatively low conductivity of Ti. Despite the bending and twisting stress imparted on the PET membrane/Au thin-film, their conductivities remained far greater than the Au thin-film on glass, (5.12×10^5 S m^{-1} compared to 1.92×10^5 S m^{-1}, respectively), as discussed in the following subsection.

3.3.1 Conductivity of PET/Au under Convex bending

Typically, conductivity is expected to increase in a flexible electronic material until stress causes the thin-film to fail (e.g. cracks, breaking). The influence of film stresses on the conductivity was determined by bending the PET membranes at different radii of curvature (1-5 mm) in a convex (Figure 3.6) manner with respect to the Au film while monitoring the impedance of the electrodes with a 10 mVrms AC signal swept from 0.01 to 60 kHz at varying DC bias voltages (Figure 3.7). The average conductivity of the Au was 4.5x105 S m-1 in the absence of curvature. As the convex curvature stress was increased, the average conductivity also increased to 4.8x105 S m-1 at an R = 1 mm. Overall, the convex bending caused the conductivity to increase by 5 - 7%, with a slight decrease ($< 2\%$) with an increasing DC bias (Figure 3.8). The slight decrease in conductivity with an increase in bias voltage is likely due to joule heating causing a loss between flat and R = 1 mm and analyzed at each R in order to assess the reproducibility and reliability of the Au layer (Figure 3.9). A decrease of less than 4% in conductivity was observed at later cycles.

3.3.2 Conductivity of PET/Au under Concave Bending

The effect of stress on concave bending (Figure 3.10), however, was not similar to convex bending, but rather resulted in a decreased conductivity for the Au film (Figure 3.11). At a 0.6 V bias, the conductivity decreased by 14% from $4.6x10^5$ S m^{-1} to $4.0x10^5$ S m^{-1} when the PET film is bent concavely to R = 1 mm. Reducing the DC bias increased the conductivity slightly due to less joule heating (Figure 3.11 and Figure 3.12). Opposite behavior in conductivity was observed with the electrodes bent at concave side when compared to electrodes at convex side. With concave bending of the electrode, shear

Figure 3.6 Convex bending of PET/Au. (■ PET Membrane, ■ Gold).
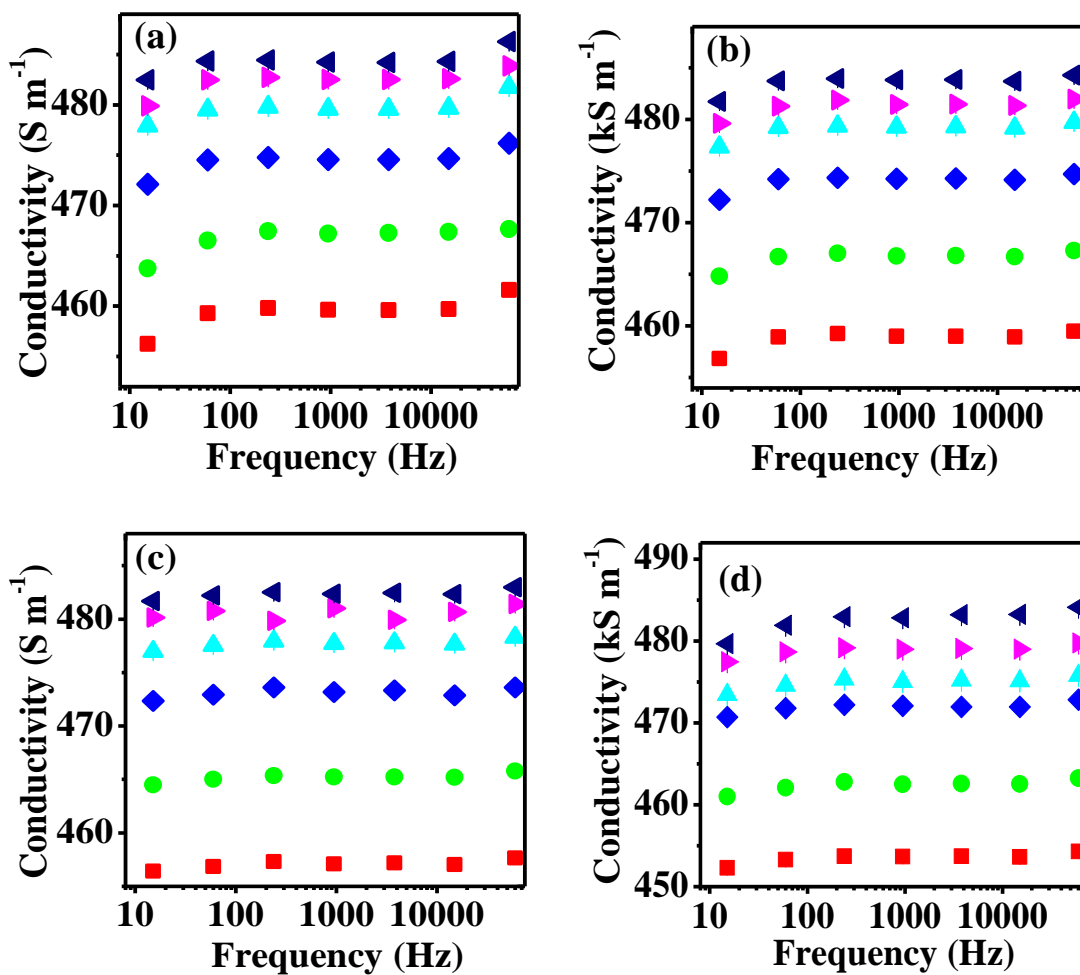
Figure 3.7 Conductivity of convexly bent PET/Au membrane at an applied frequency range for a different bias conditions: (a) 0.0 V. (b) 0.2 V. (c) 0.4 V. (d) 0.6 V. (■ Flat, ● 5 mm, ◆ 4 mm, ▲ 3 mm, ▶ 2 mm, ◀ 1 mm).
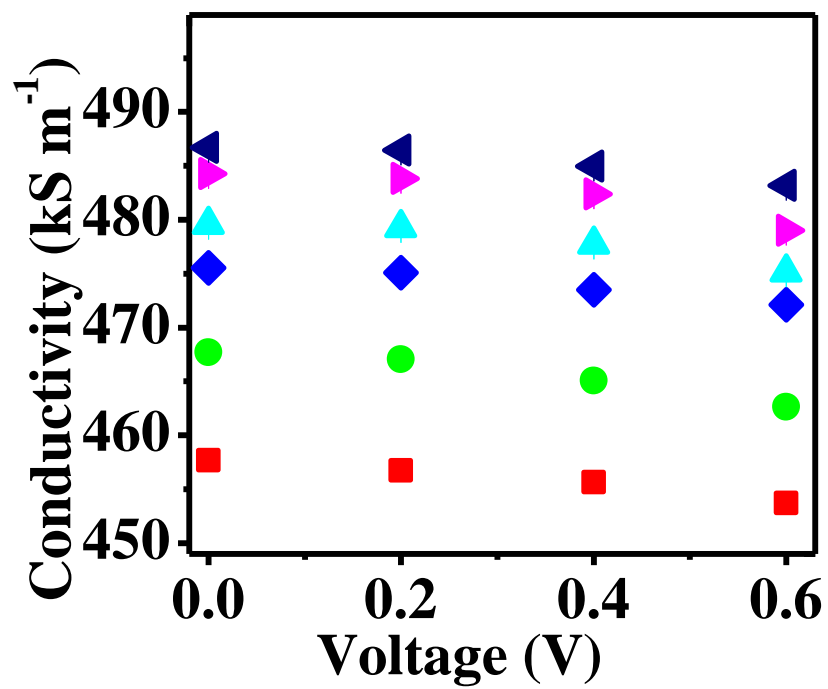
Figure 3.8 Conductivity of convexly bent PET/Au at different bias voltages. (■ Flat, ● 5 mm, ◆ 4 mm, ▲ 3 mm, ▶ 2 mm, ◀ 1 mm).
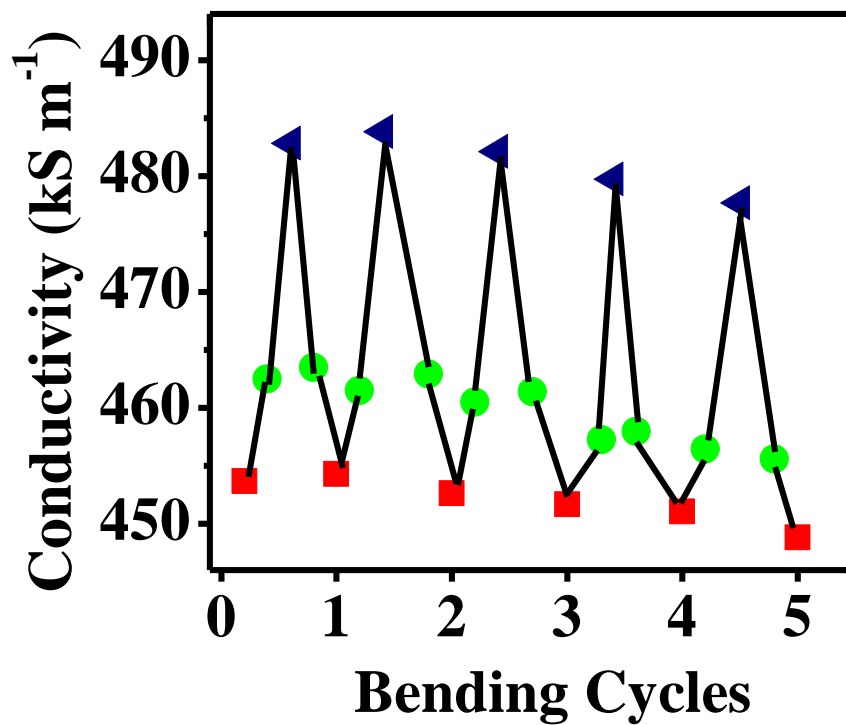
Figure 3.9 Variation of conductivity of convexly bent PET/Au with bending cycle. (■ Flat, ● 5 mm, ◄ 1 mm).

Figure 3.10 Concave bending of PET/Au. (■ PET Membrane, ■ Gold).
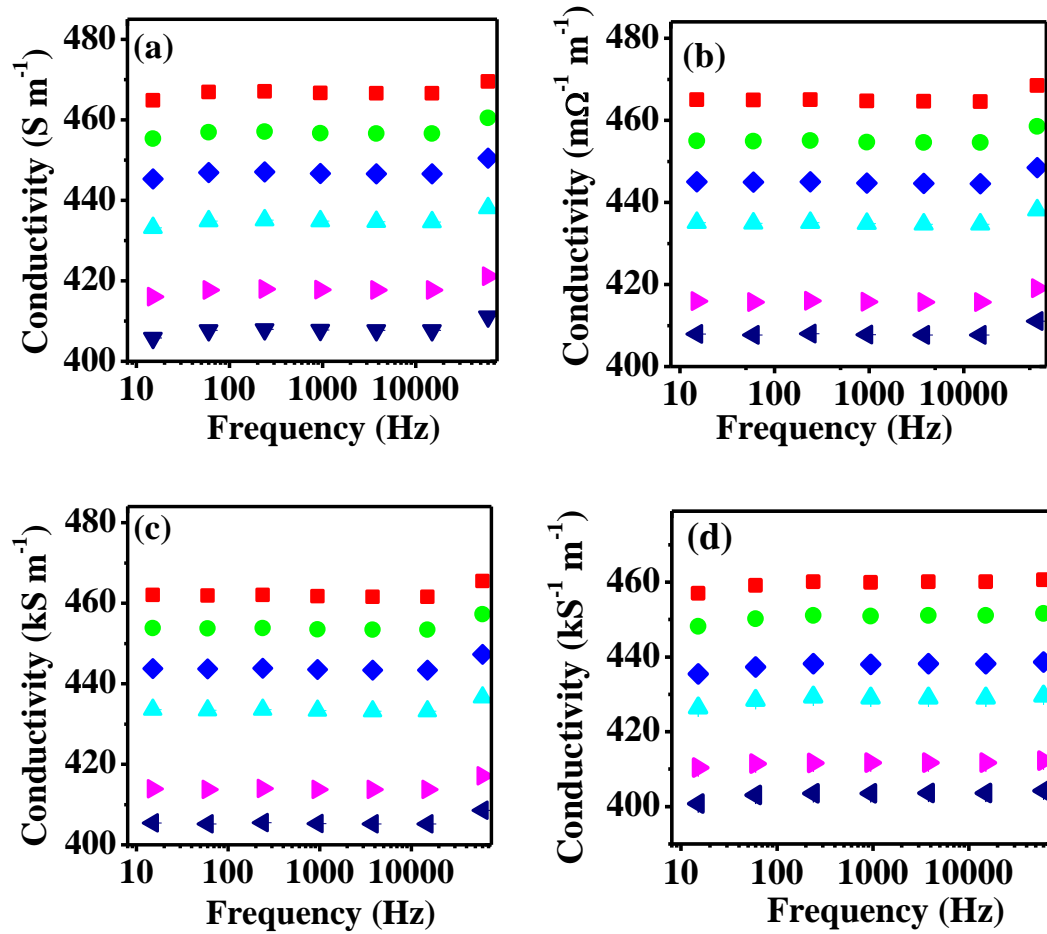
Figure 3.11 Conductivity of concave bent PET/Au membrane at an applied frequency range (a) 0.0 V. (b) 0.2 V. (c) 0.4 V. (d) 0.6 V. (■ Flat, ● 5 mm, ◆ 4 mm, ▲ 3 mm, ▶ 2 mm, ◀ 1 mm).
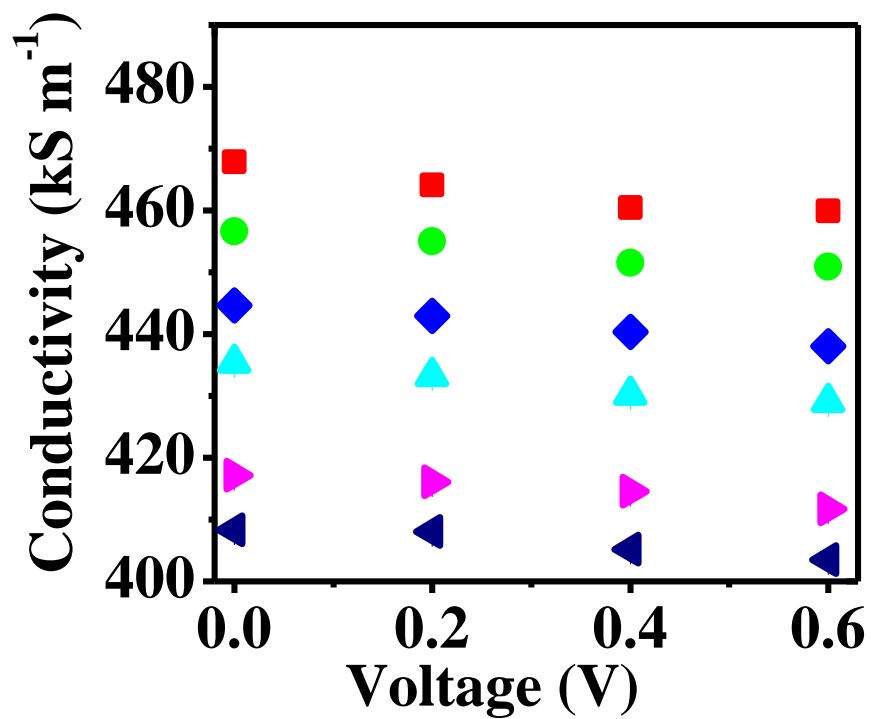
Figure 3.12 Conductivity of concave bent PET/Au at different bias voltages. (■ Flat, ● 5 mm, ◆ 4 mm, ▲ 3 mm, ▶ 2 mm, ◀ 1 mm)
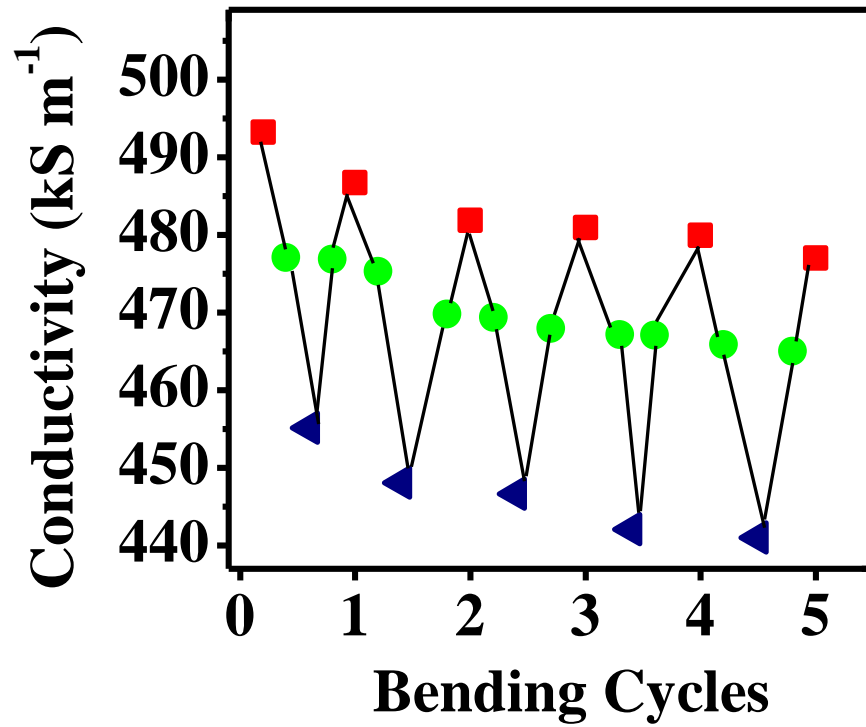
Figure 3.13 Variation of conductivity of concave bent PET/Au with bending cycle. (■ Flat, ● 5 mm, ◀ 1 mm).

stress developed resulting in an increase in the depth of the pores. This geometrical

increase in the dimension of the pores increases the size of the defects and dislocations of

the Au electrode. These defects and dislocations decrease the mobility of the electrons in

the Au thin-film and hence, a decrease in conductivity was observed. Figure 3.12 shows

the behavior of conductivity with an increase in bias voltages. The conductivity behavior

was found to be similar to the conductivity behavior of the electrodes when bent at

convex side. Repeated cycles of the concave bending (Figure 3.13) resulted in a

decreasing conductivity similar to convex bending, but with a greater decrease in

conductivity (approx. 3%) after five cycles.

3.3.3 Conductivity of PET/Au when Twisted

The effect of planar rotation twist is also studied in which the Au electrode was

twisted along the length of the membrane (Figure 3.14) as a function of twisting angle (0°,

30°, 60° and 90°). The electrical conductivity decreased with increasing planar rotation and

increased with the bias voltage (Figure 3.15), which is similar to the results observed for the

concave bending (Figure 3.11). For a 0.6 V bias, the conductivity decreased approximately

4% from 5.4×10^5 S m^{-1} to 5.2×10^5 S m^{-1} when twisted from flat to 90° angle. Conductivity

at other biased voltages also show similar behavior. The PET membrane experiences strain

along the length of Au electrode when twisted. With increasing twist angles, the torque acting

on the Au electrode increased, thus increasing the size of defects on Au-film and decrease in

the mobility of the electrons. An increase in DC bias decrease the conductivity, same as

previous cases due to joule heating (Figure 3.16). Performing multiple cycles of the planar

rotation gradually led to a minor decrease in the conductivity (Figure 3.17). Unlike the
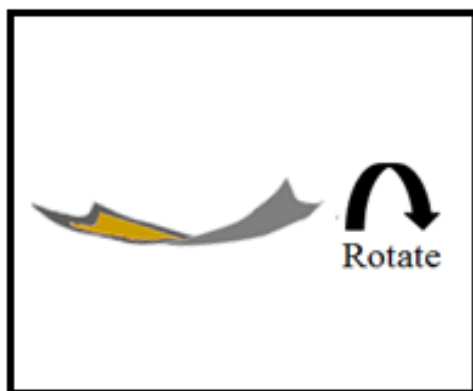
Figure 3.14 Twisted PET/Au. (■ PET Membrane, ■ Gold).
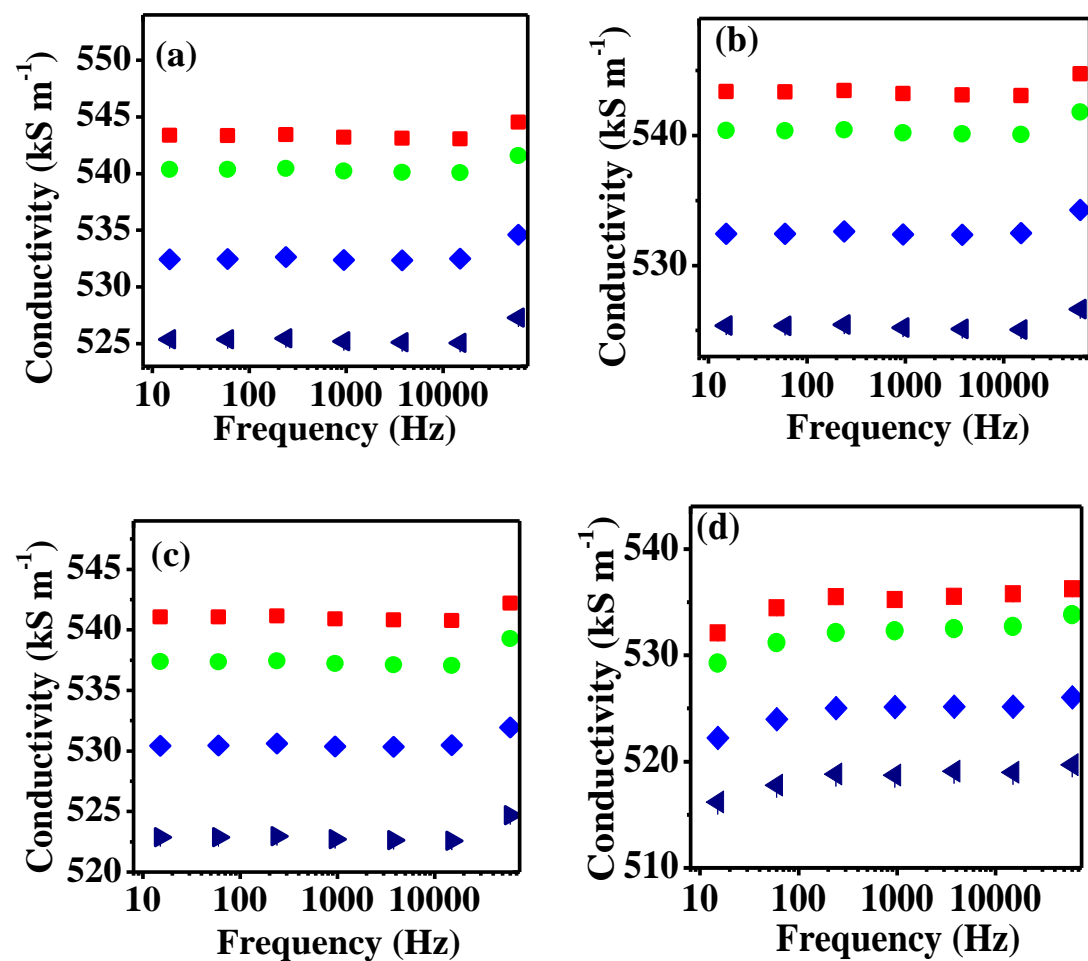
Figure 3.15 Conductivity of twisted PET/Au at (a) 0.0 V. (b) 0.2 V. (c) 0.4 V. (d) 0.6 V. (■ Flat, ● 30 °, ◆ 60 °, ◀ 90 °).
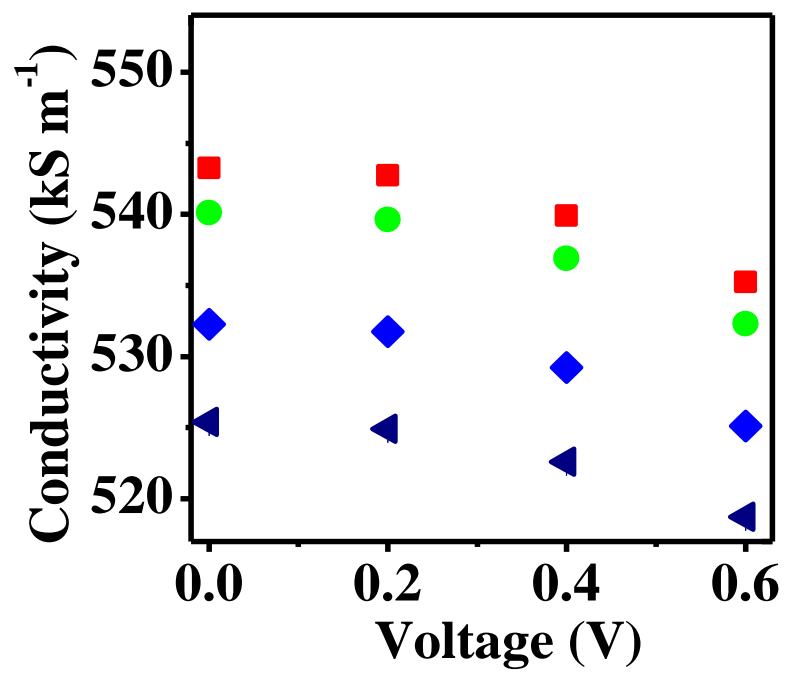
Figure 3.16 Conductivity of twisted PET/Au at different voltages. (■ Flat, ● 30 °, ◆ 60 °, ◀ 90 °).
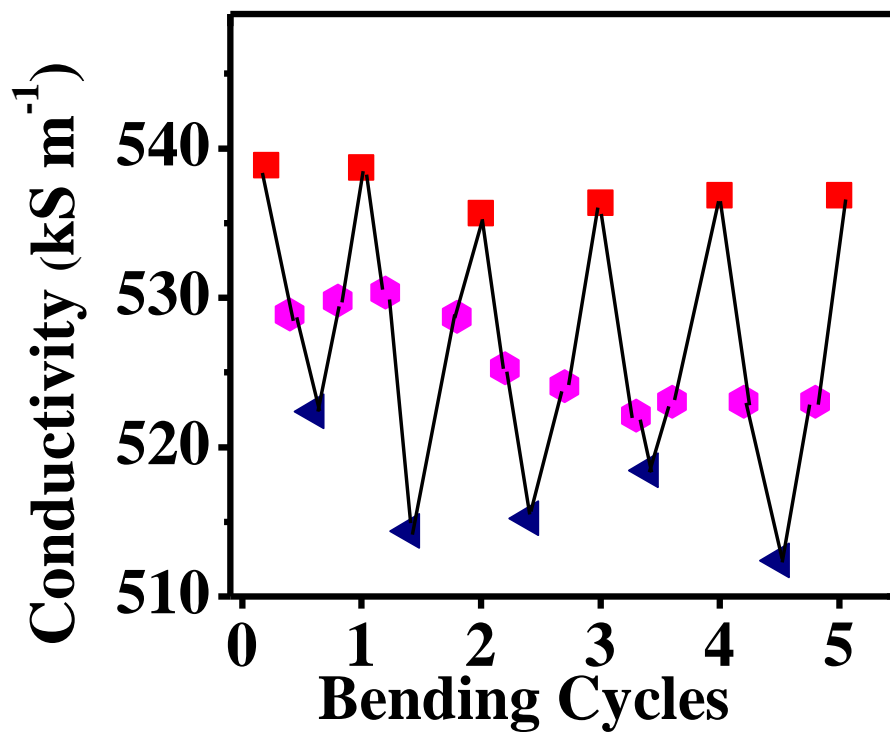
Figure 3.17 Variation of conductivity of twisted PET/Au with bending cycle. (▇ Flat, ⬢ 45 °, ◀ 90 °).

concave and convex bending, decrease of conductivity was not uniform. After 5 cycles, the conductivity decrease was only approx. 0.5% at 0°, but approx. 5% at 45° and 90°. As the PET membrane was twisted, micro-cracks were formed in the electrode, and with each twist cycle these micro-cracks grew in size to some extent, introducing relatively small variations in the measured conductivity. Thus, due to the formation of micro-cracks with increasing number of twist-cycles, a decrease in the conductivity was observed.

3.4 Response to Different Ionic Concentrations

Since this device is envisioned as a possible component for a wearable sensor, an assessment of its capabilities to measure ionic solutions was carried out. The capability of this device to measure sodium (Na^+) and potassium (K^+) ions using the electrodes as a potentiometric ion sensor was tested. These ions are two examples of ions that are secreted in human sweat. The voltage response at varying physiological concentrations (10-500 mM) of NaCl and KCl solutions was measured. The PET/Au electrode surface was silanized exposing a constant Au surface, thus confirming the interaction area of the ionic solutions and Au surface to be constant. Counter electrode and working electrode were connected to two ends of two Au electrodes and ionic solutions were aspirated such that it bridged the two separate Au electrodes. Enclosed Ag/AgCl reference electrode filled in 4 mM KCl solution was dipped in the ionic solutions. A 0.5 mA DC bias current was applied and the concentration of ionic solutions was changed for every 60 sec. Figure 3.18a shows voltage response with time as the concentration of the Na^+ solutions was changed on PET/Au membrane when flat and concavely bent at an R = 5 mm. Figure 3.18b shows the relationship between the measured voltage and the change in concentration of the Na^+ electrolyte solutions. Similar relationship was observed for K^+

55
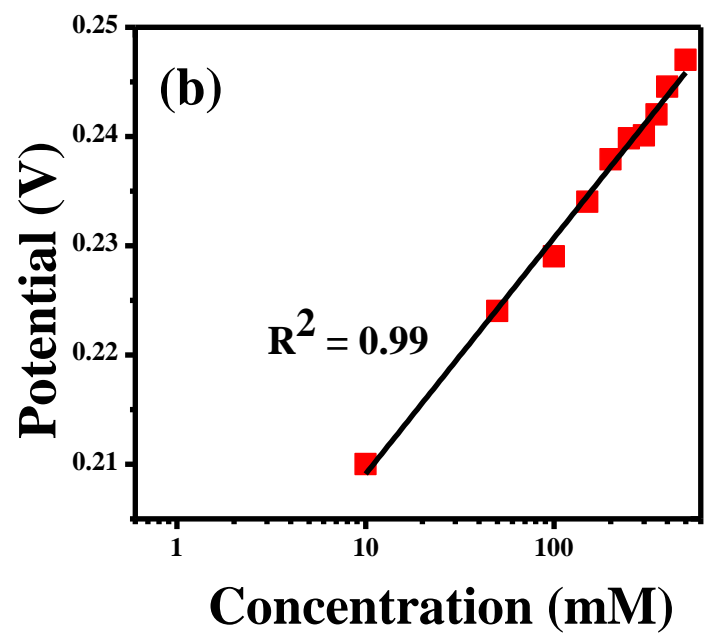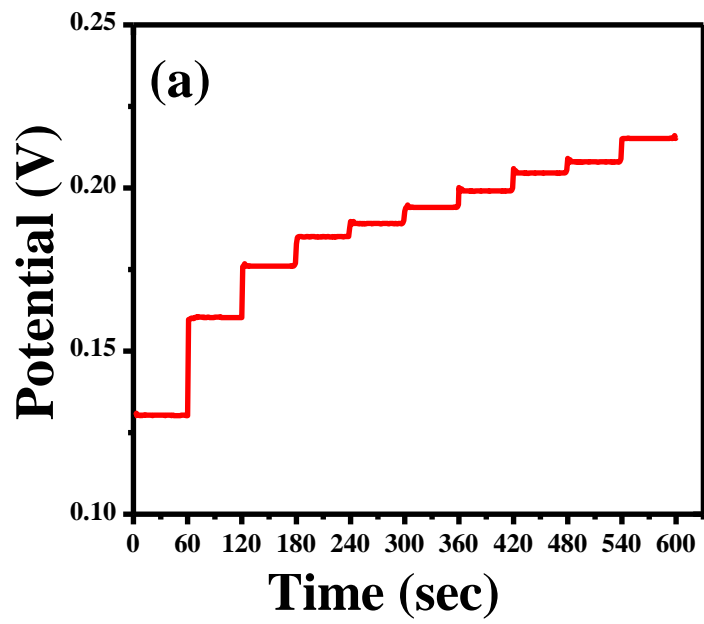
Figure 3.18 Potentiometric measurement of Na+ solution on 5 mm convex bend PET/Au. (a) Potentiometric response with time. (b) Potentiometric response with respect to concentrations.
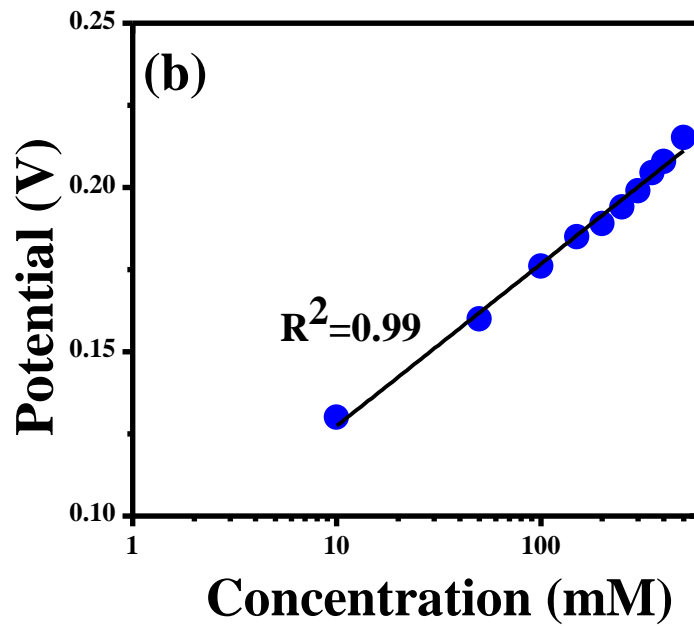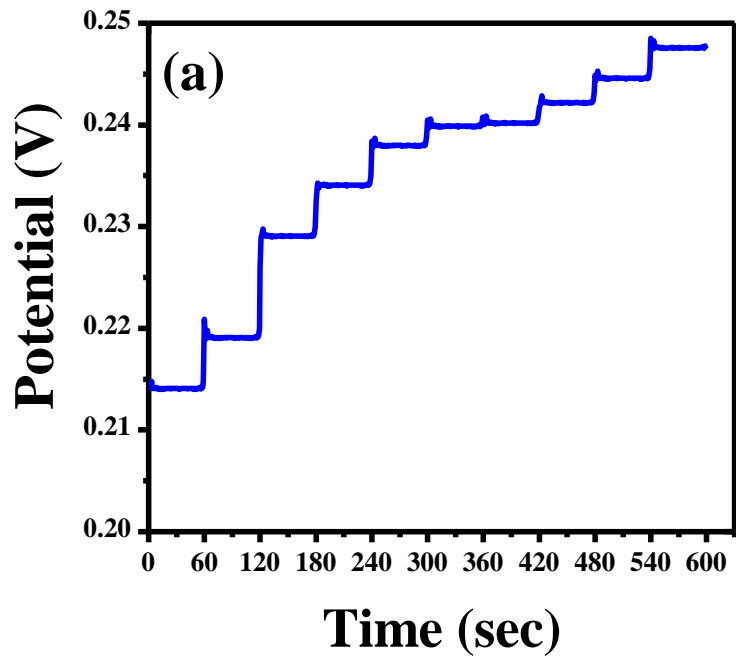
Figure 3.19 Potentiometric measurement of K+ solution on 5 mm convex bend PET/Au. (a) Potentiometric response with time. (b) Potentiometric response with respect to concentrations.

solution. (Figure 3.19) Figure 3.18 and figure 3.19 also show the electrode response to varying concentration of ionic solutions. As expected, the potential increases with increasing concentrations of the ionic solutions. These potentiometric measurements show the possibility of using the porous PET/Au membrane as an ion-selective electrode.

3.5 Conclusion

It is found that in non-porous PET membrane, the Au electrode was ruptured when it was bent to radius of curvature of 3 mm or smaller. In contrast, porous PET membrane substrates can withstand harsh mechanical loading (radius of curvature down to 1 mm and multiple bending cycles) while maintaining stable electrical properties and relatively large conductivities. When the flexible thin-film electronic system is compared with other published flexible electronic systems, conductivities are found to be within the same range (10^3 to 10^4 S/cm) as published by Kim *et al*. [101]. Also, the porous PET/Au membrane has shown conductivities of more than 4×10^5 S m^{-1} when flat as well as when it is subjected to mechanical loading (bending) and twist angles of up to 90°. It is observed that flat porous PET/Au membrane thin-film produces higher conductivities (> 2.5 times) than the same design of 50 nm thin-film gold electrodes on glass substrate. The porous PET membrane device also shows robust conductivity behavior throughout the battery of tests that it was subjected to, showing overall changes of 7% or less. In the future, this flexible electrode could be integrated in wearable devices where it could produce similar robust results under bending and other type of conditions that wearable flexible electronic apparatuses are commonly exposed to.

CHAPTER 4: ELECTRICAL CHARACTERIZATION OF CELLS

Electrical characterization of bio-particles is one of the most promising methods for label-free, real-time, and non-invasive biological detection [102]. Recently, impedance characterization of biological cells is emerging as an investigating tool for diagnosing the electrophysiological and biophysical changes in viral infections [103], cancer detection [104], and drug response [105]. The physiological behavior of the cells and their molecular expressions have significant effect on the cell membrane and cytoplasm conductivity and dielectric constant which affects the overall impedance characteristics of the cells [106]. Impedance measurement can reveal the pathological status of cells, yielding information on the effect of infections, drugs, environmental parameters, and toxicity on the cells.

4.1 Advantage of Impedance Measurement

Current techniques for analyzing cells include flow cytometry and microscopic imaging [107-108]. In general, these techniques rely upon the antibodies and ligands to detect cell membrane antigens or receptors, that are unique to the cell types. Detection procedure requires fluorescent, chemiluminescent or radioactive labeling which may be damaging to cells, causing loss of important biological information. To overcome these shortcomings, cell impedance analysis is becoming an effective method for label-fee, non-invasive biological measurement [109-111]. Various studies have demonstrated that

the cell-impedance measurements provide information on the cell behavior [112-114]. Cellular activities such as cell adhesion and spreading (cell growth) on microelectrode surfaces are sensed by measuring the induced capacitance and/or resistance changes in the electrical impedance techniques [115-116]. In 1984, Giaever and Keese reported, for the first time, the electric cell-substrate impedance sensing technique [117]. Since then this technique has continuously being improved and refined [118-120]. In recent years, impedance-based sensing systems were used for monitoring drug-induced activities of different types of carcinoma cells for drug discovery [121-132].

The electric properties of biological cells due to the Maxwell–Wagner effect [133] can be obtained by evaluating the dielectric relaxation of their suspensions [134-135]. This technique has been used to study the real-time monitoring of cellular growth, differentiation, proliferation and metabolism [136]. At low frequency, electrical current tends to go around the cell rather than penetrating through it. Thus, the pathological change that takes place inside the cell cannot be determined. However, high frequency reduces the electrical shielding effect and the double layer effect [137], thus decreasing the capacitive impedance of the cell and increasing the electric field through the cell. This can be used to obtain the impedance characteristics of the cell at various pathological states and identify unhealthy cells from the healthy cells for detection of many medical condition.

4.2 Cell Induction and Differentiation

P19 cells, as mentioned in Chapter 2, can be differentiated into anyone of the three germ type (cell) by specific treatments. Therefores, undifferentiated P19 cells when
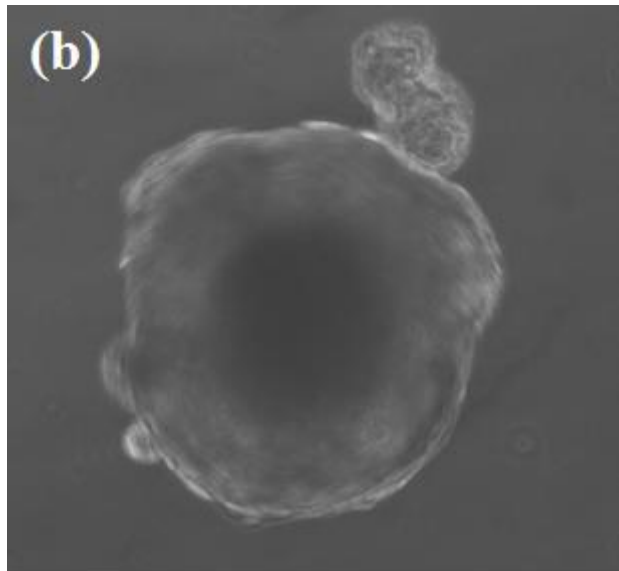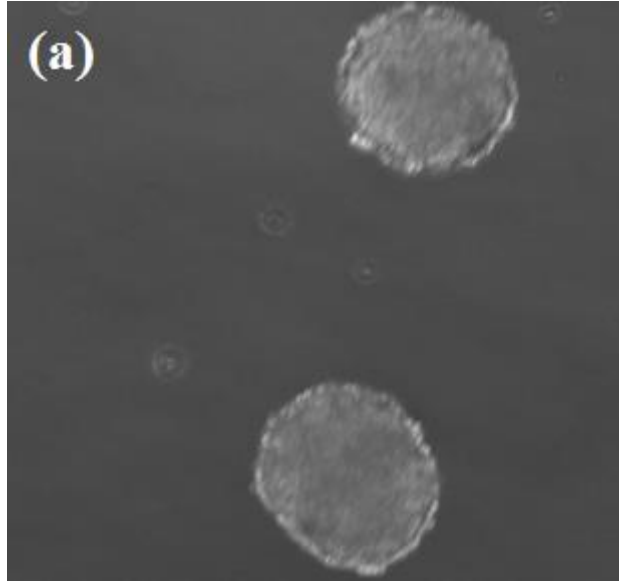
Figure 4.1 Aggregated cells in induction media for neural differentiation (a) Day 2. (b) Day 4.
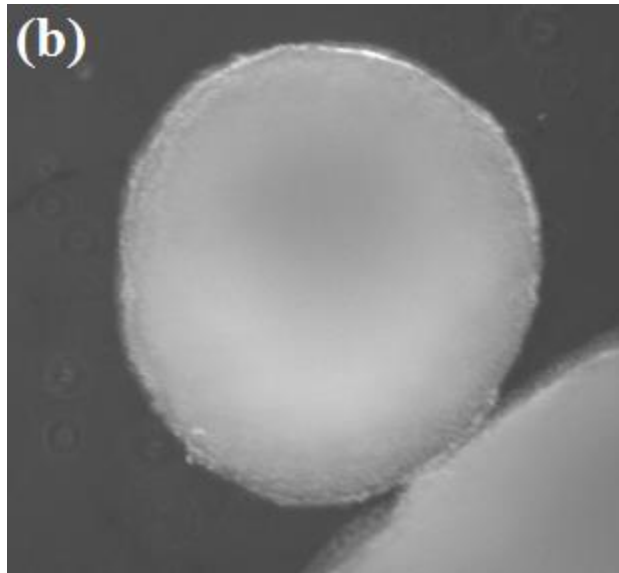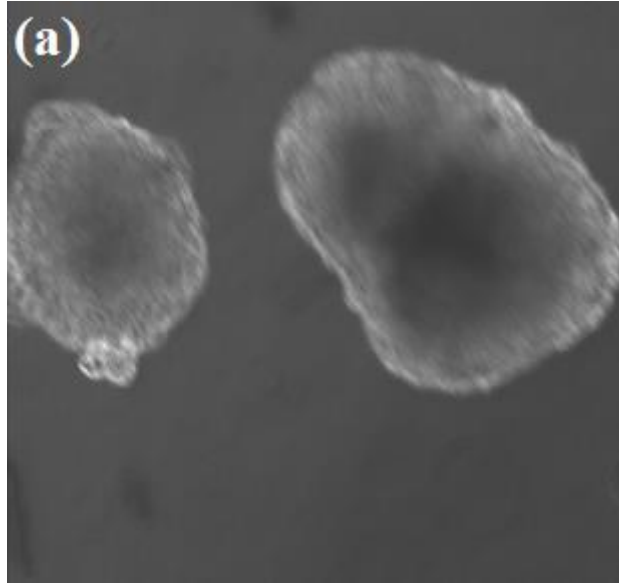
Figure 4.2 Aggregated cells in induction media for cardiomyocyte differentiation (a) Day 2. (b) Day 4.
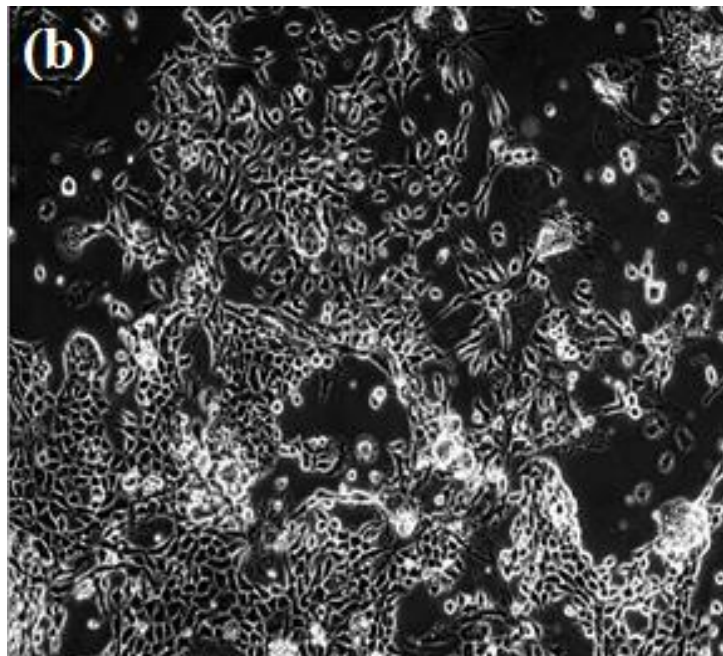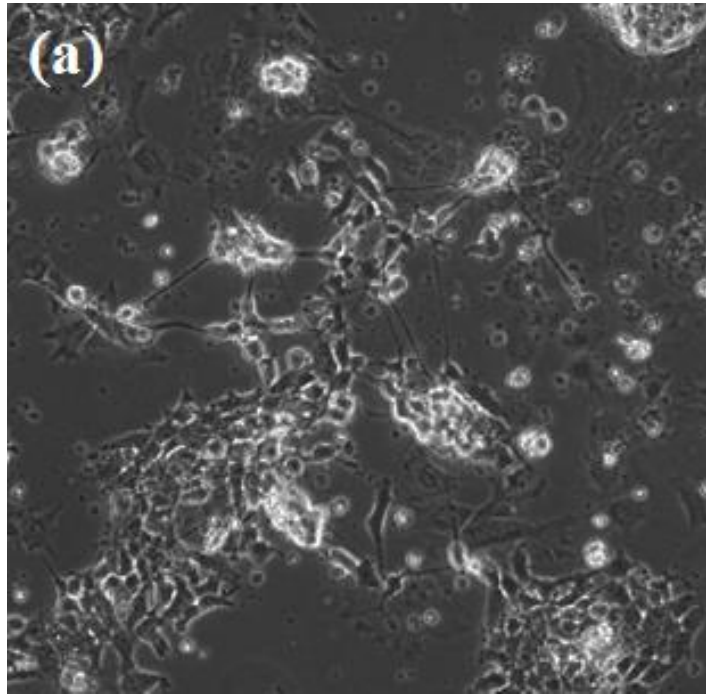
Figure 4.3 Differentiated cells on Day 7 (a) Neuronal cells. (b) Cardiomyocytes cells.

treated with retinoic acid could induce into neuronal cells and when treated with dimethyl sulfoxide (DMSO), they are induced into cardiac and skeleton muscle cells. Both the treatment processes are very similar. In this work, non-adhesive bacteriological culture dish was treated with F127 solution in 1x PBS at concentration of 1:100 for an hour, followed by a PBS rinse. Undifferentiated single cells, at high density (~10^5 cells/ml), were plated on the dish and cultured in induction media for 4 days. For neuronal differentiation, induction media consists of CGM supplemented with 5 % FBS and 2mM retinoic acid prepared in 95% ethanol. For cardiac differentiation, induction media was prepared by mixing CGM supplemented with 10% FBS and 1% DMSO. They aggregate to form spheroid shaped structures during this induction period (Figure 4.1 and Figure 4.2). On day 2, induction media and the spheroids were transferred into a conical flask, very gently and cautiously so as not to break the spheroids. Supernatant in the conical flask was replaced with fresh induction media without disturbing the spheroids and transferred to fresh F127 treated bacteriological dish as discussed earlier. On day 5, both types of induced spheroids were dispersed in trypsin to dissociate into single cells. Dissociated single cells were plated on culture substrate and cultured in CGM for differentiation. By day 8, one can observe formation of neurite like structure confirming differentiation process (Figure 4.3). It may take upto day 10 to obtain fully mature differentiated cells.

4.3 Measurement Experiment

To measure the impedance of the differentiated cells, the induced cells were plated on the flexible MEA device. Prior to plating the cells, gold electrode surfaces were

coated with FN for 1.5 hours, as earlier discussed in chapter 2, followed by Dulbecco's

PBS wash. Dissociated single cells were then plated on the gold electrodes and allowed

to adhere on the electrode surface for 24 hours under standard culture conditions, as

mentioned earlier. For 12 hours CGM was replaced with fresh media. After 48 hours,

neurite like structures were formed on the cultured cells and change in morphology was

observed (Figure 4.3).

4.3.1 Electrical Characterization

The impedance measurement of the differentiated cells was performed with a

three-step procedure. First, the impedance measurement of the microelectrodes was

carried out in the CGM prior to cell seeding in order to obtain the baseline data. For the

second step, the impedance measurement was performed after the surfaces of the

microelectrodes were coated with FN deposition. The final measurement was conducted

when the FN coated gold electrodes were covered with differentiated P19 cells (Neuronal

and Cardiomyocyte) after seeding. The entire set of measurements (cell–free baseline,

cell–free FN–coated electrodes, and cells-covered electrode) were recorded separately

using a set of flexible MEA devices which consistently demonstrated the same cell–free

baseline impedance characteristics.

A sinusoidal signal of 10 mV$_{rms}$ was applied between the sensing electrodes.

Frequency was varied from 60 kHz to 10 Hz. A DC bias voltage of 0.5 V was applied for

all the measurements. No change in impedance was observed between FN coated and

uncoated electrodes. This shows that the FN coating add no impedance on the electrodes,
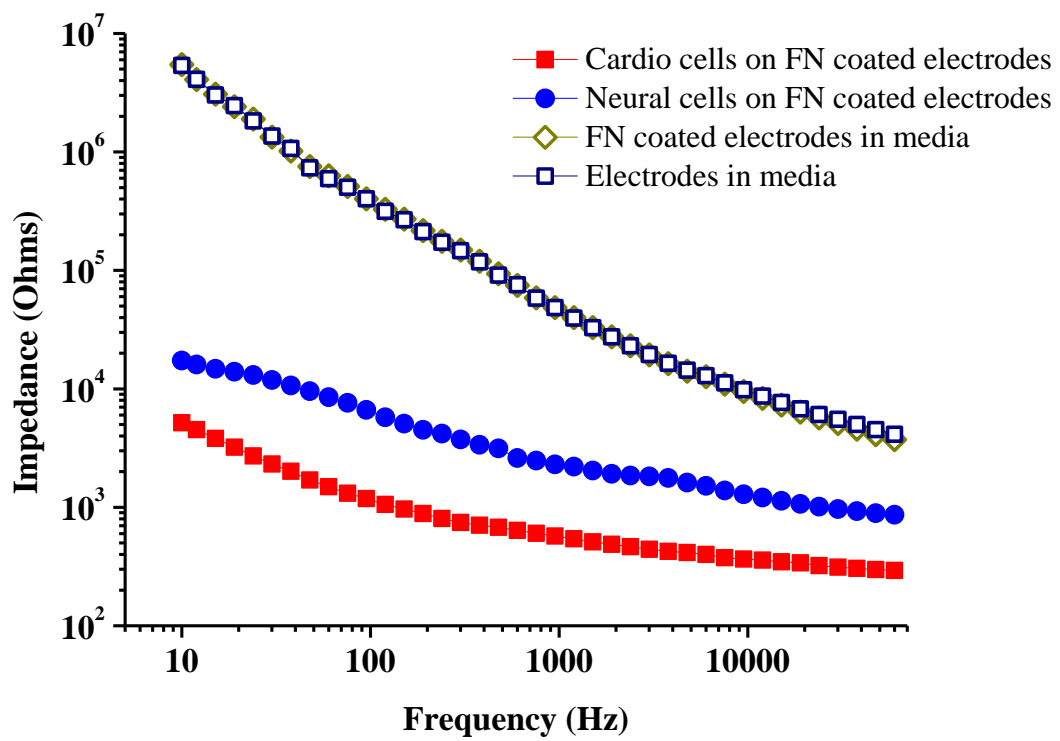
Figure 4.4 Measured impedance of electrodes with and without cells.
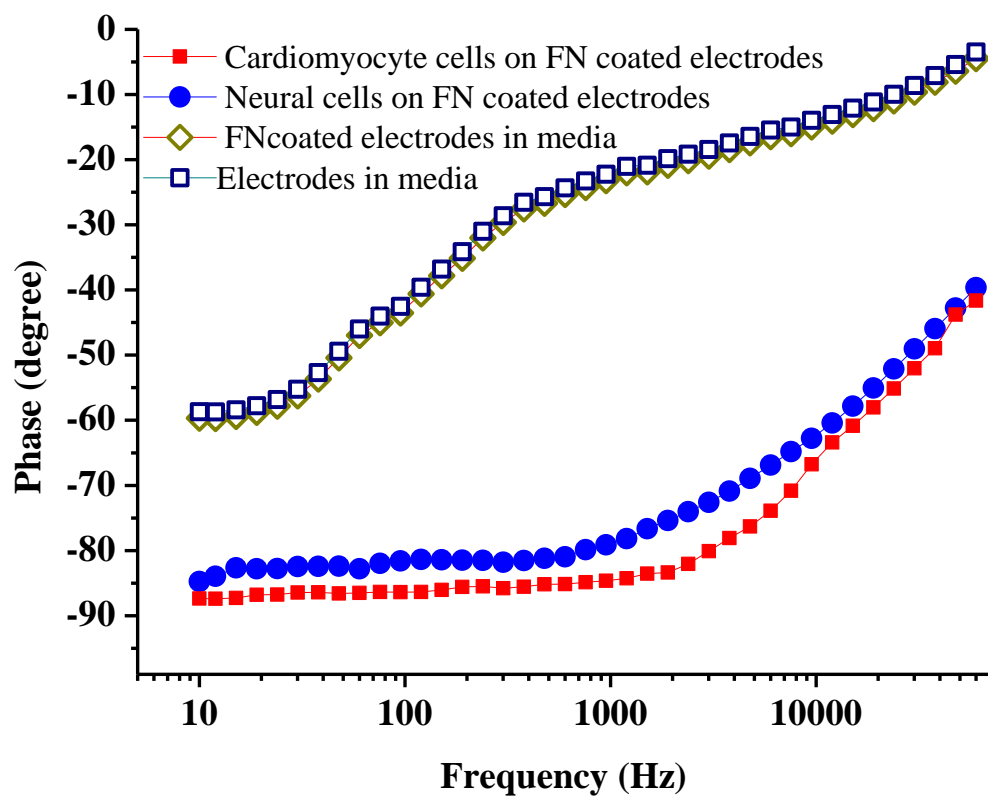
Figure 4.5 Phase angle of electrodes with and without cells.
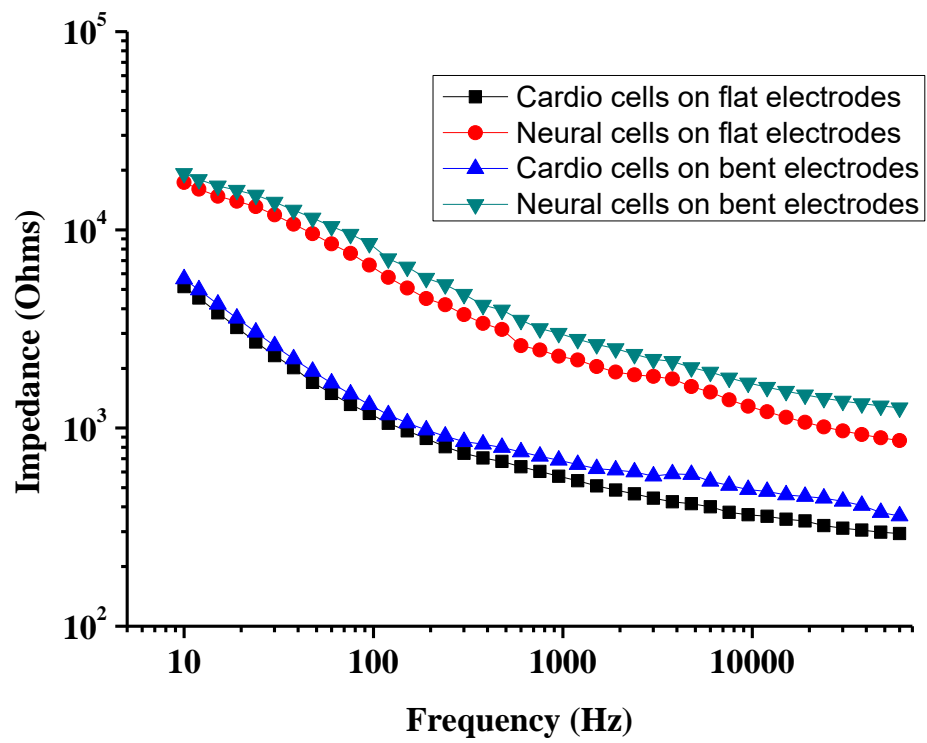
Figure 4.6 Phase angle of electrodes with and without cells.

which is advantageous for the system. With cells adhered to the gold electrodes, measured impedance was reduced by 3 orders of magnitude for the cardiomyocyte cells and by 2 orders of magnitude for the neuronal cells (Figure 4.4). At low frequency, high impedance was measured as high effective capacitive nature of the cells tends to block the low frequency, forcing the current to flow around the cells, as explained earlier. This capacitive behavior was confirmed with phase angle measurement which shows phase to be between -80 ° and -90 ° (Figure 4.5). At high frequency low impedance was measured as the current penetrates through the cells (as discussed earlier). A decrease in phase angle was observed which confirmed lowering of the capacitive nature of the cells at high frequency. Figure 4.6 shows impedance of the FN coated gold electrodes with each type of the cells when the PET membrane was flat and bent at R = 1 mm. Measured impedance were comparable when flat and bent, maintaining the electrical stability as already discussed in chapter 2. Since different cells cytoplasm have different permittivity and conductivity, these results show that, on the porous flexible PET/Au device, not only the cell impedance can be measured but based on the measured impedance different types of cells can be identified. Since healthy and unhealthy cells will have different impedance, this method will be able to distinguished between them.

4.4 Conclusion

The methodology demonstrated here shows the possibility of using flexible PET/Au MEA device for impedance based measurement to sense the electrical responses of the cells. Such measurements are helpful to distinguish between healthy and unhealthy cells. Procedure discussed here, illustrates differentiation of P19 cells on the flexible

MEA device. A decrease in the impedance of the microelectrode with cells shows the possibility of using electrical characterization of cells on the porous flexible MEA, as a way to find the viability and other cellular-properties. Comparable cell impedance measurement when the PET membrane was flat and bent reconfirm electrical stability of this system under mechanical loading conditions. This gives rise to the feasibility of measuring cellular network structures in order to understand complex interconnections occurring during cell-cell communication, in a system that could, to some extent, emulate *in-vivo* conditions.

CHAPTER 5: CONCLUSION AND FUTURE WORK

In this work, flexible polymer based MEA is used to electrically position the cells, against gravity, on microelectrodes. DEP conditions were optimized not only to trap the cells but to maintain the viability of the trapped cells for cellular activity. It was found experimentally that high trapping frequency ruptured the cell membrane. Frequency was optimized just enough for strong DEP trapping but not to have any effect on the cell membrane. Layer-by-layer adsorption of hCAM on the microelectrodes shows strong adherence between the cells and the electrode surface. When incubated under proper culture conditions the cells have long time viability (more than 48 hours). Viability of cells on flexible material suggest this type of device could be used for *in-vivo* studies of mammalian cell behavior in the future.

For flexible PET membrane, which was etched to create pores, the flexibility of the deposited gold electrode was better when compared to having no pores. Stable electrical properties under harsh mechanical stress-strain conditions were maintained. The applied stress-strain mostly concentrated around the pores, as confirmed with formation of cracks, thus protecting a majority of the microelectrode surface area from further rupture or any extreme mechanical deterioration. Porous PET/Au microelectrode is capable of measuring response to different solutions and different physiological concentration of ions that are found in body-fluids. Demonstration of potentiometric

measurement to different concentration of Na and K ions show the possibility of these porous PET/Au for use as a wearable device material, if the electrodes are modified for ion selective detection and demonstrate Nernst behavior.

The cells were also characterized on the porous PET/Au MEA device. Cells were differentiated on the device and impedance of the electrodes with cells were measured which showed measurable variation compared to the electrodes without cells. This creates a possibility of distinguishing different types of cells by measuring cell-impedance on the porous flexible device. Thus, various cell analyses could be performed by measuring cell responses under different biological conditions and that could be applied to a wide number of applications.

Future work will, attempt the formation of 3-D spheroid type structure of trapped cells to reproduce complex cellular networks, usually found in mammalian tissue. Such attempt could provide with more in-depth understanding of cellular behavior in a format that start to approach the *in* vivo structure.

An in-depth investigation into the interfacial characteristic and mechanism of gold electrodes on porous PET membrane under different stress-strain conditions is required. Also, besides characterizing the cell by measuring electrical impedance, it would be of immense interest to measure action potential of the cells on the porous flexible electrodes. This would open the possibility of using an implanted device for monitoring real-time, continuous long-term cell activity including erratic short-term responses.

REFERENCES

1. S. N. Bhatia, U. J. Balis, M. L. Yarmush, and M. Toner., "Effect of cell-cell interactions in preservation of cellular phenotype: cocultivation of hepatocytes and nonparenchymal cells", *FASEB J.*, 1999, Vol. 13, pp. 1883.

2. V. Hasirci, and H. Kenar., "Novel surface patterning approaches for tissue engineering and their effect on cell behavior", *Nanomedicine*, 2006, Vol. 1, pp.73.

3. J. H. Lee, H. E. Kim, J. H. Im, Y. M. Bae, J. S. Choi, K. M. Huh, and C. S. Lee., "Preparation of orthogonally functionalized surface using micromolding in capillaries technique for the control of cellular adhesion", *Colloids Surf. B: Biointerfaces*, 2008, Vol. 64, pp. 126.

4. F. Garnier, R. Hajlaoui, A. Yassar, and P. Srivastava., "All-polymer field-effect transistor realized by printing techniques", *Science.*, 1994, Vol. 265, pp. 1684.

5. Z. Bao, Y. Feng, A. Dodabalapur, V. R. Raju, A. J. Lovinger, "High-performance plastic transistors fabricated by printing techniques"., *Chemistry of Materils.*, 1997, Vol. 9, pp. 1299.

6. R. Langer, and J. P. Vacanti., "Tissue engineering", *Science.*, 1993, Vol. 260, pp. 920.

7. N. Patel, R. Padera, G. H. Sanders, S. M. Cannizzaro, M. C. Davies, R. Langer, C. J. Roberts, S. J. Tendler, P. M. Williams, and K. M. Shakesheff., "Spatially controlled cell engineering on biodegradable polymer surfaces", *FASEB J.*, 1998, Vol. 12, pp. 1447.

8. B. D. Boyan, T. W. Hummert, D. D. Dean, and Z. Schwartz., "Role of material surfaces in regulating bone and cartilage cell response", *Biomaterials.*, 1996, Vol. 17, pp. 137.

9. A. S. Curtis, and C. D. Wilkinson, "Reactions of cells to topography", *J Biomaterials Science. Polymer Edition.*, 1998, Vol. 9, pp. 1313.

10. R. T. Tranquillo., "Self-organization of tissue-equivalents: the nature and role of contact guidance", *Biochemical Society Symposium.*, 1999, Vol. 65, pp. 27.

11.   M. D. Evans, and J. G. Steele., "Polymer surface chemistry and a novel attachment mechanism in corneal epithelial cells", *J Biomedical Materials Research*, 1998, Vol. 40, pp. 621.

12.   Y. J. van der Zijpp, A. A. Poot, and J. Feijen., "ICAM-1 and VCAM-1 expression by endothelial cells grown on fibronectin-coated TCPS and PS", *J Biomedical Materials Research A*. 2003, Vo. 65 pp. 51.

13.   R. E. Baier, V. A. Depalma, D. W. Goupil, and E. Cohen., "Human platelet spreading on substrata of known surface chemistry", *J Biomedical Materials Research*., 1985, Vol. 19, pp. 1157.

14.   W. S. Ramsey, W. Hertl, E. D. Nowlan, and N. J. Binkowski., "Surface treatments and cell attachment", *In Vitro*., 1984. Vol. 20, pp. 802.

15.   T. A. Horbett, M. B. Schway, and B. D. Ratner., "Hydrophilic-hydrophobic copolymers as cell substrates: Effect on 3T3 cell growth rates", *J Colloid and Interface Science*., 1985, Vol. 104, pp. 28.

16.   M. Mrksich, C. S. Chen, Y. Xia, L. E. Dike, D. E. Ingber, and G. M. Whitesides., "Controlling cell attachment on contoured surfaces with self-assembled monolayers of alkanethiolates on gold", *Proceeding of the National Academy of Sciences USA.,* 1996, Vol. 93, pp. 10775.

17.   S. Kidambi, I. Lee, and C. Chan., "Controlling primary hepatocyte adhesion and spreading on protein-free polyelectrolyte multilayer films", *J American Chemical Society*., 2004, Vol. 126, pp16286.

18.   J. D. Mendelsohn, S. Y. Yang, J. Hiller, A. I. Hochbaum, and M. F. Rubner., "Rational design of cytophilic and cytophobic polyelectrolyte multilayer thin films", *Biomacromolecules*., 2003, Vol. 4, pp. 96.

19.   M. J. Dalby, M. O. Riehle, H. Johnstone, S. Affrossman, and A. S. G. Curtis., "In vitro reaction of endothelial cells to polymer demixed nanotopography", *Biomaterials*., 2002, Vol. 23, pp. 2945.

20.   C. D. W. Wilkinson, M. Riehle, M. Wood, J. Gallagher, and A. S. G. Curtis., "The use of materials patterned on a nano- and micro-metric scale in cellular engineering", *Material Science and Engineering C*., 2002, vol. 19, pp. 263.

21.   H. Tsutsui, E. Yu, S. Marquina, B. Valamehr, I. Wong, H. Wu, and C. M. Ho., "Efficient dielectrophoretic patterning of embryonic stem cells in energy landscapes defined by hydrogel geometries", *Annals of Biomedical Engineering*., 2010, Vol. 38, pp. 3777.

22.   D. S. Gary, J. L. Tan, J. Voldman, and C. S. Chen., "Dielectrophoretic registration of living cells to a microelectrode array", *Biosensors and Bioelectronics*., 2004, Vol. 19, pp. 1765.

23.   D. F. Chen, H. Du, and W. H. Li., "A 3D paired microelectrode array for accumulation and separation of microparticles", *Journal of Micromechanics and Microengineering*, 2006, Vol. 16, pp. 1162.

24.   G. W. Gross, A. Harsch, B. K. Rhoades, and W. Gopel, "Odor, drug and toxin analysis with neuronal networks in vitro: Extracellular array recording of network responses", *Biosensors and Bioelectronics*., 1997, Vol. 12, pp. 373.

25.   J. C. Chang, G. J. Brewer, and B. C. Wheeler, "Microelectrode array recordings of patterned hippocampal neurons for four weeks", *Biomed. Microdevices*, 2000, Vol. 2, pp. 245.

26.   R. Segev, M. Benveniste, E. Hulata, N. Cohen, A. Palevski, E. Kapon, Y. Shapira, and E. Ben-Jacob, "Long term behavior of lithographically prepared in vitro neuronal networks", *Phys. Rev. Lett*., 2002, Vol. 88, pp. 102.

27.   G. W. Gross, "Simultaneous single unit recording in vitro with a photoetched laser deinsulated gold multimicroelectrode surface", *IEEE Trans. Biomed. Eng*., 1979, Vol. 26, pp. 273.

28.   J. Pine., "Recording action potentials from cultured neurons with extracellular microcircuit electrodes", *J. Neuroscience Methods*., 1980, Vol. 2, pp. 19.

29.   K. L. Drake, K. D. Wise, J. Farraye, D. J. Anderson, and S. L. BeMent, "Performance of planar multisite microprobes in recording extracellular single-unit intracortical activity", *IEEE Trans. Biomed. Eng*., 1988, Vol. 35, pp. 719.

30.   Y. Jimbo, H. P. C. Robinson, and A. Kawana, "Simultaneous measurement of intracellular calcium and electrical activity from patterned neural networks in culture", *IEEE Trans. Biomed. Eng*., 1993, Vol. 40, pp. 804.

31.   M. P. Maher, J. Pine, J. Wright, and Y. C. Tai, "The neurochip: A new multielectrode device for stimulating and recording from cultured neurons", *J. Neuroscience Methods*., 1999, Vol. 87, pp. 45.

32.   J. L. Novak, and B. C. Wheeler, "Multisite hippocampal slices recording   and stimulation using a 32 elements microelectrode array", *J Neuroscience Methods.,* 1988, Vol. 23, pp. 149.

33.   U. Egert, B. Schlosshauer, S. Fennrich, W. Nisch, M. Fejtl, T. Knott, T. Muller, and H. Hammerle., "A novel organotypic long-term culture of the rat hippocampus on substrate-integrated multielectrode arrays", *Brain Research Brain Research Protocols*., 1998, Vol. 2, pp. 229.

34.   P. Thiebaud, C. Beuret, M. Koudelka-Hep, M. Bove, S. Martinoia, M. Grattarola, H. Jahnsen, R. Rebaudo, M. Balestrino, J. Zimmer, and Y. Dupont., "An array of Pt-tip microelectrodes for extracellular monitoring of activity of brain slices", *Biosensors and Bioelectronics*., 199, Vol. 14, pp. 61.

35.   D. E. Clapham, A. Shrier, R. L. DeHaan., "Junctional resistance and action potential delay between embryonic heart cell aggregates", *J General Physiology*., 1980, Vol. 75, pp. 633.

36.   H. Haemmerle, U. Egert, A. Mohr, and W. Nisch., "Extracellular recording in neuronal networks with substrate integrated microelectrode arrays", *Biosensors and Bioelectronics*., 1994, Vol. 9, pp. 691.

37.   P. Igelmund, B. K. Fleischmann, I.R. Fischer, J. Soest, O. Gryshchenko, M. M. Boehm-Pinger, H. Sauer, Q. Liu, and J. Hescheler, "Action potential propagation failures in long-term recordings from embryonic stem cell-derived cardiomyocytes in tissue culture", Pfluegers Archiv., 1999, Vol. 437, pp. 669.

38.   W. Nisch, J. Böck, U. Egert, H. Haemmerle, and M. Mohr., "A thin film microelectrode array for monitoring extracellular neuronal activity in vitro", *Biosensors and Bioelectronics*., 1994, Vol. 9, pp. 737.

39.   J. Pine, M. Maher, S. Potter, Y. C. Tai, S. Tatic-Lucic, and J. Wright, "A cultured neuron probe", *IEEE Engineering in Medicine and Biology Society*., 1997. Vol. 5, pp. 2133.

40.   A. Stett, W. Barth, S. Weiss, H. Haemmerle, and E. Zrenner., "Electrical multisite stimulation of the isolated chicken retina", *Vision Research*., 2000 Vol. 40, pp. 1785.

41.   C. A. Thomas Jr, P. A. Springer, G. E. Loeb, Y. Berwald-Netter, and L. M. Okun., "A miniature microelectrode array to monitor the bioelectric activity of cultured cells", *Experimental Cell Research*., 1972, Vol. 74, pp. 61.

42.   G. W. Gross, A. N. Williams, and J. H. Lucas, "Recording of spontaneous activity with photoetched microelectrode surfaces from mouse spinal neurons in culture", *J. Neuroscience Methods*., 1982, Vol. 5, pp.13.

43. W. G. Regehr, J. Pine, C. S. Cohan, M. D. Mischke, and D. W. Tank., "Sealing cultured invertebrate neurons to embedded dish electrodes facilitates long- term stimulation and recording", *J. Neuroscience Methods*., 1989, Vol. 30, pp. 91.

44. P. Connolly, P. Clark, P., A. S. Curtis, J. A. Dow, and C. D Wilkinson., "An extracellular microelectrode array for monitoring electrogenic cells in culture", *Biosensors and Bioelectronics*., 1990, Vol. 5, pp. 223.

45. A. S. Curtis, L. Breckenridge, P. Connolly, J. A. Dow, C. D. Wildinson, and R. Wilson, "Making real neural nets: design criteria", *Medical and Biological Engineering and Computing*., 1992, Vol. 30, pp. CE33.

46. J. C. Chang, G. J. Brewer, and B. C. Wheeler, "Modulation of neural network activity by patterning", *Biosensors and Bioelectronics*., 2001, Vol. 16, pp. 527.

47. M. G. Lagally., "Silicon nanomembranes", *MRS Bulletin.,* 2007, Vol. 32, pp. 57

48. J. A. Rogers, M. G. Lagally, and R. G. Nuzzo., "Synthesis, assembly and applications of semiconductor nanomembranes", *Nature* 2011, Vol. 477, pp. 45.

49. D. H. Kim, J. H. Ahn, W. M. Choi, H. S. Kim, T. H. Kim, J. Z. Song, Y. G. Y. Huang, Z. J. Liu, C. Lu, and J. A. Rogers., "Stretchable and foldable silicon integrated circuits', *Science* 2008, Vol. 320, pp. 507.

50. G. A. Salvatore, N. Munzenrieder, T. Kinkeldei, L. Petti, C. Zysset, I. Strebel, L. Buthe, and G. Troster., "Wafer-scale designof lightweight and transparent electronics that wraps around hairs", *Nature Communication.,* Vol. 2014, Vol. 5, pp. 2982.

51. C. L. Wang, H. L. Dong, W. P. Hu, Y. Q. Liu, and D. B. Zhu, "Semiconducting π-conjugated systems in field-effect transistors: A material adyssey of organic electronics", *Chemical Reviews.*, 2012, Vol. 112, pp. 2208.

52. S. W. Bedel, K. Fogel, P. Lauro, D. Shahrjerdi, J. A. Ott, and D. Sadana., "Layer transfer by controlled spalling", *J. Physics D: Applied Physics*., 2013, Vol. 2013, Vol. 46, pp. 152002.

53. M. Melzer, D. Makarov, A. Calvimontes, D. Karnaushenko, S. Baunack, R. Kaltofen, Y. F. Mei, and O. G. Schmidt., "Stretchable magnetoelectronics", *Nano Letter*., 2011, Vol. 11, pp. 2522.

54. D.-H. Kim, L. Nanshu, M. Rui, Y.-S. Kim, R.-H. Kim, S. Wang, J. Wu, S. M. Won, H. Tao, A. Islam, K. J. Yu, T. Kim, R. Chowdhury, M. Ying, L. Xu, M. Li, H.-J. Chung, H. Keum, M. McCormick, P. Liu, Y.-W. Zhang, F. G. Omenetto, Y.

Huang, T. Coleman, and J. A. Rogers., "Epidermal electronics", *Science.,* 2011, Vol. 333, pp. 838.

55.   D. J. Lipomi, M. Vosgueritchian, B. C. K. Tee, S. L. Hellstrom, J. A. Lee, C. H. Fox, and Z. Bao., "Skin-like pressure and strain sensors based on transparent elastic films of carbon nanotubes", *Nature Nanotechnology.*, 2011, Vol. 6, pp. 788.

56.   A. Gangopadhyay, S. Minnikanti, D. R. Reyes, M. V. Rao, and N. Peixoto., "Dielectrophoretic trapping of P19 cells on indium tin oxide based microelectrode arrays", *IEEE EMBS.*, 2013, Vol. 6, pp 941.

57.   K. Takei, T. Takahashi, J. C. Ho, H. Ko, A. G. Gillies, P. W. Leu, R. S. Fearing, and A. javey., "Nanowire active-matrix circuitry for low-voltage macroscale artificial skin", *Nature Materials.*, 2010, Vol. 9, pp. 821.

58.   W. Wu, L. Wang, Y. Li, F. Zhang, L. Lin, S. Niu, D. Chenet, X. Zhang, Y. hao, T. F. Heinz, J. Hone, and Z. L. Wang., "Piezoelectricity of single-atomic-layer MoS_2 for energy conversion and piezotronics", *Nature.*, 2014, Vol. 514, pp. 470.

59.   M. C. McAlpine, H. Ahmad, D. Wang, and J. R. Heath., "Highly ordered nanowire arrays on plastic substrates for ultrasensitive flexible chemical sensors", *Nature Materials.*, 2007, Vol. 6, pp. 379.

60.   M. Kaltenbrunner, T. Sekitani, J. Reeder, T. Yokota, K. Kuribara, M. Drack, R. Schwodiauer, I. Graz, S. Bauer-Gogonea, S. Bauer, and T. Someya., "An ultra-lightweight design for imperceptible plastic electronics", *Nature.*, 2013, Vol. 499, pp. 458.

61.   S. Xu, Y. Zhang, L. Jia, K. E. Mathewson, K-I. Jang, J. Kim, H. Fu, X. Huang, P. Chava, R. Wang, S. Bhole, L. Wang, Y. J. Na, Y. Guan, M. Flavin, Z. Han, Y. Huang, and J A. Rogers., "Soft microfluidic assemblies of sensors, circuits, and radios for the skin", *Science.*, 2014, Vol. 344, pp. 70.

62.   C. Wang, D. Hwang, Z. Yu, K. Takei, J. Park, T. Chen, B. Ma, and A. Javey., "User-interactive electronic skin for instantaneous pressure visualization", *Nature Materials.*, 2013, Vol. 12, pp. 899.

63.   J. Liang, L. Li, X. Niu, Z. Yu, and Q. Pei., "Elastomeric polymer light-emitting devices and displays", *Nature Photon*. 2013, Vol. 7, pp. 817.

64.   Z. Sonner, E. Wilder, J. Heikenfeld, G. Kasting, F. Beyette, D. Swaile, F. Sherman, J. Joyce, N. Kelley-Loughnane, and R. Nail, "The microfluidics of the

eccrine sweat gland, including biomarker partitioning, transport, and biosensing implications", *Biomicrofluidics*., 2015, Vol. 9, pp. 031301.

65. W. Gao, S. Emaminejad, H. Y. Y. Nyein, S. Challa, K. Chen, A. Peck, H. M. Fahad, H. O. H. Shiraki, D. Kiriya, D.-H. Lien, G. A. Brooks, R. W. Davis, and A. Javey., "Fully integrated wearable sensor arrays for multiplexed in situ perspiration analysis", *Nature*., 2016, Vol. 529, pp. 509.

66. P. R. C. Gascoyne, and Jody Vykoukal., "Particle separation by dielectrophoresis." *Electrophoresis*., 2002, Vol. 23, pp. 1973.

67. H. Tsutsui, and C. M. Ho., "Cell separation by non-inertial force fields in microfluidic systems," *Mechanics Research Communications*., 2009, Vol. 36, pp. 92.

68. C. F. Gonzalez, and V. T. Remcho, "Harnessing dielectric forces for separations of cells, fine particles and macromolecules," *Journal of Chromatography A*., 2005, Vol. 1079, pp. 59.

69. H. Morgan, M. P. Hughes, and N. G. Green, "Separation of submicron bioparticles by dielectrophoresis," *Biophysical Journal*., 1999, Vol. 77, pp. 516.

70. E. B. Cummings, and A. K. Singh, "Dielectrophoresis in microchips containing arrays of insulating posts: Theoretical and experimental results," *Analytical Chemistry*., 2003, Vol. 75, pp. 4724.

71. H. A. Pohl., "Dielectrophoresis the behavior of neutral matter in nonuniform electric fields", *Cambridge University Press. Cambridge*., 1978.

72. T. B. Jones., "Electromechanics of particles", *Cambridge University Press. Cambridge*., 1995.

73. P. Gravesan, J. Branebjerg, and O. S. Jensen, "Microfluidics: A review", *Journal Micromech. Microengg*., 1993, Vol. 3, pp. 168.

74. L. Kim, M. D. Vahey, H. Y. Lee, and J. Voldman, "Microfluidic arrays for logarithmically perfused embryonic stem cell culture", *Lab on a Chip*., 2006, Vol. 6, pp. 394.

75. B. H. Jo, L. M. V. Lerberghe, K. M. Motsegood, and D. J. Beebe, "Three-dimensional micro-channel fabrication in polydimethylsiloxane (PDMS) elastomer," *Journal of Microelectromechanical Systems*., 2000, Vol. 9, pp. 76.

76. W. Chen, and T. J. McCarthy, "Layer-by-layer deposition: A tool for polymer surface modification," *Macromolecules*., 1997, Vol. 30, pp. 78.

77. J. P. DeRocher, P. Mao, J. Han, M. F. Rubner, and R.E. Cohen, "Layer-by-layer assembly of polyelectrrolytes in nanofluidic devices," *Macromolecules*., 2010, Vol. 43, pp. 2430.

78. S. P. Forrey, D. R. Reyes, M. Gaitan, and L. E. Locascio, "Cellular immobilization within microfluidic microenvironments: Dielectrophoresis with polyelectrolyte multilayers," *Journal of the American Chemical Society*., 2006, Vol. 128, pp. 13678.

79. D. R. Reyes, J. S. Hong, J. T. Elliott, and M. Gaitan., "Hybrid cell adhesive material for instant dielectrophoretic cell trapping and long-term cell function assessment," *Langmuir*., 2011, Vol. 27, pp. 10027.

80. M. Melzer, J. I. Monch, D. Makarov, Y. Zabila, G. S. C. Bermudez, D. Karnaushenko, S. Baunack, F. Bahr, C. Yan, M. Kaltenbrunner, and O. G. Schmidt., "Wearable magnetic field sensors for flexible electronics" *Advanced Materials*., 2015, Vol. 27, pp. 1274.

81. Y. Chen, J. Au, P. Kazlas, A. Ritenour, H. Gates, and M. McCreary., "Electronic paper: Flexible active-matrix electronic ink display", *Nature*., 2003, Vol. 423, pp. 136.

82. S. Kim, H.-J. Kwon, S. Lee, H. Shim, Y. Chun, W. Choi, J. Kwack, D. Han, M. Song, S. Kim, S. Mohammadi, S. Kee, and S. Y. Lee., ""Low-power flexible organic light-emitting diode display device", Advanced *Materials*., 2011, Vol. 23, pp. 3511.

83. M.-C. Choi, Y. Kim, and C.-S. Ha, "Polymers for flexible displays: from material selection to device applications", *Progress in Polymer Science.,* 2008, Vol. 33, pp. 581.

84. H. Gleskova, I.-C. Cheng, S. Wagner, J. C. Sturm, and Z. Suo., "Mechanics of thin-film transistors and solar cells on flexible substrates", *Solar Energy*., 2006, Vol. 80, pp. 687.

85. C. J. Brabec, N. S. Sariciftic, and J. C. Hummelen., "Plastic solar cells", *Advancd Functional Materials* 2001, Vol. 11, pp. 15.

86. L. Dong, C. Xu, Y. Li, C. Wu, B. Jiang, Q. Yang, E. Zhou, and F. Kang., "Simultaneous production of high-performance flexible textile electrodes and

fiber electrodes for wearable energy storage", *Advanced Materials*., 2016, Vol. 28, pp. 1675.

87. C.-T. Huang, C.-L. Shen, C.-F. Tang, and S.-H. Chang., "A wearable yarn-based piezo-resistive sensor", *Sensors and Actuators A*, 2008, Vol. 141, pp. 396.

88. J. Q. Liu, Z. Y. Zeng, X. H. Cao, G. Lu, L. H. Wang, Q. L. Fan, W. Huang, and H. Zhang., "Preparation of MoS_2-polyvinylpyrrolidone nanocomposites for flexible nonvolatile rewritable memory devices with reduced graphene oxide electrodes", *Small*., 2012, Vol. 8, pp. 3517.

89. J. Q. Liu, Z. Y. Yin, X. H. Cao, F. Zhao, L. H. Wang, W. Huang, and H. Zhang., "Fabrication of fexible, all-reduced graphene oxide non-volatile memory devices", *Advanced Materials*., 2013, Vol. 23, pp. 233.

90. Q. Y. He, H. G. Sudibya, Z. Y. Yin, S. X. Wu, H. Li, F. Boey, W. Huang, P. Chen, and H. Zhang., "Centimeter-long and large-scale micropatterns of reduced graphene oxide films: fabrication and sensing applications", *ACS Nano*., 2010, Vol. 4, pp. 3201.

91. A. Weber, S. Deutschben, A. Plichta, and A. Habeck., "Thin glass-polymer systems as flexible substrates for displays", *SID*., 2002, Vol. 33, pp. 53.

92. H. S. Shin, J. B. Koo, J. K. Jeong, Y. G. Mo, H. K. Chung, J. H. Cheon, J. H. Choi, K. M. Kim, J. H. Hur, S. H. Park, S. K. Kim, and J. Jang., "4.1 inch top-emission AMOLED on flexible metal foil"., *SID*., 2005, Vol. 36, pp. 1642.

93. B.-J. Kim, H.-A.-S. Shin, I.-S. Choi, and Y.-C. Joo., "Electrical failure and damage analysis of multi-layer metal films on flexible substrate during cyclic bending deformation", *ISTFA*., 2011, Vol. 37, pp. 13.

94. J. R. Greer, W. C. Oliver, and W. D. Nix., "Size dependence of mechanical properties of gold at the micron scale in the absence of strain gradients"., *Acta Materialia*., 2005, Vol. 53, pp. 1821.

95. M. Lewandowska, and K. J. Kurzydyowski., "Thermal stability of a nanostructured aluminium alloy"., *Materials Characterization*., 2005, Vol. 55, pp. 395.

96. A. Mathur, and J. Erlebachera, "Size dependence of effective Young's modulus of nanoporous gold", *Applied Physics Letetrs*., 2007, Vol. 90, pp. 061910.

97. J. Herrmann, K-H. Müller, T. Reda, G. R. Baxter, B. Raguse, G. J. J. B. de Groot, R. Chai, M. Roberts, and L. Wieczorek., "Nanoparticle films as sensitive strain gauges", *Applied Physics Letters*., 2007, Vol. 91, pp. 183105.

98. D. S. Gianola, S. V. Petegem, M. Legros, S. Brandstetter, H. V. Swygenhoven, and K. J. Hemker., "Stress-assisted discontinuous grain growth and its effect on the deformation behavior of nanocrystalline aluminum thin films" *Acta Materialia*., 2006, Vol. 54, pp. 2253.

99. M. Legros, D. S. Gianola, and K. J. Hemker., "In situ TEM observations of fast grain-boundary motion in stressed nanocrystalline aluminum films", *Acta Materialia*., 2008, Vol. 56, pp. 3380.

100. S. Hong, and S. Myung., "Nanotube Electronics: A flexible approach to mobility", *Nature Nanotechnology*., 2007, Vol. 2, pp. 207.

101. Y. Kim, J. Zhu, B. Yeom, M. Di Prima, X. Su, J.-G. Kim, S. J. Yoo, C. Uher, and N. A. Kotov, "Stretchable nanoparticle conductors with self-organized conductive pathways", *Nature*., 2013, Vol. 500, pp. 59.

102. J. Wegener, C. R. Keese, and I. Giaever., "Electric cell-substrate impedance sensing (ECIS) as a noninvasive means to monitor the kinetics of cell spreading to artificial surfaces", *Experiment Cell Research*., 2000, Vol. 259, pp. 158.

103. M. H. McCoy, and E. Wang., "Use of electric cell-substrate impedance sensing as a tool for quantifying cytopathic effect in influenza a virus infected MDCK cells in real-time", *J Virological Methods*., 2005, Vol. 130, pp. 157.

104. P. Aberg, I. Nicander, J. Hansson, P. Geladi, U. Holmgren, and S. Ollmar., "Skin cancer identification using multifrequency electrical impedance – a potential screening tool", *IEEE Transactions on Bio-medical Engineering*., 2004, Vol. 51, pp. 2097.

105. X. Huang, D. W. Greve, D. D. Nguyen, and M. M. Domach., "Impedance based biosensor array for monitoring mammalian cell behavior", *IEEE Sensors*., 2003, Vol. 1, pp. 304.

106. L. Yang, L. R. Arias, T. S. Lane, M. D. Yancey, and J. Mamouni., "Real-time electrical impedance-based measurement to distinguish oral cancer cells and non-cancer oral epithelial cells", *Analytical and Bioanalytical Chemistry*., 2011, Vol. 399, pp. 1823.

107. G. Boeck., "Current status of flow cytometry in cell and molecular biology", *International Review of Cytology*., 2001, Vol. 204, pp. 239.

108. D. A. Basiji, W. E. Ortyn, L. Liang, V. Venkatachalam, and P. Morrissey., "Cellular image analysis and imaging by flow cytometry"., *Clinics in Laboratory Medicine*., 2007, Vol. 27, pp. 653.

109. K. H. Gilchrist, L. Giovangrandi, and G.T.A. Kovacs., "Analysis of microelectrode-recorded signals from a cardiac cell line as a tool for pharmaceutical screening", *Transducer*., 2001, pp. 390.

110. R. Schmukler, G. Johnson, J.Z. Bao, and C.C. Davis., "Electrical impedance of living cells: a modified four electrode approach", *IEEE Engineering in Medicine and Biology Society*., 1988, Vol. 10, pp. 899.

111. J. Z. Bao, C. C. David, and R. E. Schmukler., "Impedance spectroscopy of human erythrocytes: system calibration and nonlinear modeling", *IEEE Transactions on Bio-medical Engineering*., 1993, Vol. 40, pp. 364.

112. H. P. Schwan., "Electrical properties of tissue and cell suspensions: mechanisms and models"., *Advances in Biological and Medical Physics*., 1957, Vol. 5, pp. 147.

113. S. Takashima, K. Asami, and Y. Takahashi., "Frequency domain studies of impedance characteristics of biological cells using micropipet technique. I. Erythrocyte", *Biophysics J*., 1988, Vol. 54, pp. 995.

114. H. E. Asami, and K. S. Zhao, "Dielectric measurement of a single sub-millimeter size microcapsule", *Colloid and Polymer Science*., 1994, Vol. 272, pp. 64.

115. R. Ehret, W. Baumann, M. Brischwein, A. Schwinde, K. Stegbauer, and B. Wolf., "Monitoring of cellular behavior by impedance measurements on interdigitated electrode structures", *Biosensors and Bioelectronics*., 1997, Vol. 12, pp. 29.

116. R. Ehret, W. Baumann, M. Brischwein, A. Schwinde, and B. Wolf., "On-line control of cellular adhesion with impedance measurements using interdigitated electrode structures", *Medical and Biological Engineering and Computing*., 1998, Vol. 36, pp. 365.

117. I. Giaever, and C. R. Keese., "Monitoring fibroblast behavior in tissue culture with an applied electric field", *Proc Natl Acad Sci*., 1984, Vol. 81 pp. 3761.

118. I. Giaever, and C. R. Keese., "Micromotion of mammalian cells measured electrically", *Proc Natl Acad Sci*., 199, Vol. 88, pp. 7896.

119. I. Giaever, and C. R. Keese., "Toxic cells can tell", *Chemtech*., 1992, Vol. 22, pp. 116.

120. I. Giaever, and C. R. Keese., "A morphological biosensor for mammalian cells", *Nature*.,1993, Vol. 366, pp. 591.

121. K. Solly, X. Wang, X. Xu, B. Strulovici, and W. Zheng., "Application of real-time cell electronic sensing (RT_CES) technology to cell-based assays", *Assay and Drug Development Technology*., 2004, Vol. 2, pp. 363.

122. P. Linderholm, J. Vannod, Y. Barrandon, and P. Renaud., "Bipolar resistivity profiling of 3D tissue culture", *Biosensors and Bioelectron*ics., 2007, Vol.22, pp. 789.

123. R. McGuinness., "Impedance-based cellular assay technologies: recent advances, future promise", *Current Opinion in Pharmacology*., 2007, Vol. 7, pp. 535.

124. B. D. Klo, R. Kurz, H. G. Jahnke, M. Fischer, S. Rothermel, U. Anderegg, J. C. Simon, and A. A. Robitzki., "Microcavity array (MCA)-based biosensor chip for functional drug screening of 3D tissue models", *Biosensors and Bioelectronics*., 2008, Vol. 23, pp. 14730.

125. Y. Chen, J. Zhang, Y. Wang, L. Zhang, R. Julien, K. Tang, N. Balasubramanian., "Real-time monitoring approach: assessment of effects of antibodies on the adhesion of NCI-H460 cancer cells to the extracellular matrix", *Biosensors and Bioelectronics*., 2008, Vol. 23, pp. 1390.

126. Q. Liu, J. Yu, L. Xiao, J. C. O. Tang, Y. Zhang, P. Wang, and M. Yang., "Impedance studies of bio-behavior and chemosensitivity of cancer cells by micro-electrode arrays", *Biosensors and Bioelectronics*., 2009, Vol. 24, pp. 1305.

127. G. Park, C. K. Choi, A. E. English, and T. E. Sparer., "Electrical impedance measurements predict cellular transformation", *Cell Biology International*., 2009, Vol. 33, pp. 429.

128. H. E. Ayliffe, A. B. Frazier, and R. D. Rabbitt., "Electric impedance spectroscopy using microchannels with integrated metal electrodes", *J Microelectromechanical System*., 1999, Vol. 8, pp. 50.

129. S. Gawad, S. Metz, L. Schild, and P. Renaud., "Impedance spectroscopy cell analysis in microchannels", *Micro Total Analysis Systems*., 2001, pp. 253.

130. S. Gawad, M. Wuthrich, L. Schild, O. Dubochet, P. Renaud, and E. Obermeier., "On-chip impedance spectroscopy of flow-cytometry using a differential electrode sensor", *Transducers*., 2001, pp. 1190.

131. Y. Huang, N. Chen, J. Borninski, and B. Rubinsky., "A novel microfluidic cell-chip for single cell analysis and manipulation", *Micro Electro Mechanical Systems*., 2003, pp. 403.

132. S. K. Mohanty, S. K. Ravula, K. L. Engisch, and A. B. Frazier., "A micro system using dielectrophoresis and electrical impedance spectroscopy for cell manipulation and analysis", *Solid State Sensors and Actuators, Transducers*., 2003, pp. 1055.

133. R. Pething, and D. B. Kell., "The passive electrical properties of biological systems: their significance in physiology, biophysics and biotechnology", *Physics in Medicine and Biology*., 1987, Vol. 32, pp. 933.

134. S. Gawad, K. Cheung, U. Seger, A. Bertsch, and P. Renaud., "Dielectric spectroscopy in a micromachined flow cytometer: theoretical and practical considerations", *Lab on a Chip*., 2004, Vol. 4, pp. 241.

135. V. L. Sukhorukov, G. Meedt, M. Kurschner, and U. Zimmermann., "A single shell model of biological cell accounting for the dielectric anisotropic of the plasma membrane", *J Electrostatic*., 2001, Vol. 50, pp. 191.

136. A. R. Heiskanen, C. F. Spegel, N. Kostesha, T. Ruzgas, and J. Emneus., "Monitoring of Saccharomyces cerevisiae cell proliferation on thiol-modified planar gold microelectrodes using impedance spectroscopy", *Langmuir*., 2008, Vol. 24, pp. 9066.

137. M. Lohndorf, U. Schlecht, T. M. A. Gronewold, A. Malave, and M. Tewes., "Microfabricated high-performance microwave impedance biosensors for detection of aptamer–protein interactions", *Applied Physics Letters*., 2005, Vol. 87, pp. 243902.

BIOGRAPHY

Aveek Gangopadhyay received his Bachelor of Engineering from University of Rajasthan, Jaipur, India in 2005. He then proceeded to pursue graduate studies in Electrical and Computer Engineering at Syracuse University, obtaining his Masters in Electrical Engineering in 2007. He later joined George Mason University for Ph.D. and worked as a Guest Researcher at National Institute of Standards and Technology, MD, USA.

At GMU, Aveek taught multiple courses and labs in the area of Circuits, Microelectronics and Semiconductors. He designed experiments for undergraduate technical labs. He was involved with undergraduate senior design groups. At NIST, his primary research area is cell trapping and flexible electronics. His areas of interest include VLSI circuit designing and fabrications and bioelectronics.